Geomorphology 255 (2016) 108–124

Contents lists available at ScienceDirect

Geomorphology

journal homepage: www.elsevier.com/locate/geomorph

Evaluating process domains in small arid granitic watersheds: Case study of Pima Wash, South Mountains, Sonoran Desert, USA

Yeong Bae Seong [a,*], Phillip H. Larson [b], Ronald I. Dorn [c], Byung Yong Yu [d]

[a] Department of Geography Education, Korea University, Anam-Dong, Seongbuk-Gu, Seoul 136-701, Republic of Korea
[b] Department of Geography, Minnesota State University, Mankato, MN 56001, USA
[c] School of Geographical Sciences and Urban Planning, Arizona State University, Tempe, AZ 85287-5302, USA
[d] AMS Laboratory, Advanced Analysis Center, Korea Institute of Science and Technology, Seoul 136-791, Republic of Korea

ARTICLE INFO

Article history:
Received 11 August 2015
Received in revised form 15 December 2015
Accepted 18 December 2015
Available online 23 December 2015

Keywords:
Disturbance
Ecosystem
Ephemeral channel
Process domains

ABSTRACT

This paper provides support for the concept of geomorphic process domains developed by Montgomery (1999) by linking geomorphic processes to ecological variations seen in the Pima arid granitic watershed of the Sonoran Desert, Phoenix, Arizona. Closer joint spacing shows a statistically significant correlation with lower percentages of mineral grain attachment as measured by digital image processing of backscattered electron microscope imagery. Lower mineral grain attachment leads to more frequent spalling of rock surfaces, as measured by varnish microlamination (VML) ages of the last spalling event. In contrast, more distant joint spacing leads to in situ ^{10}Be erosion rates of 3.4–8.5 mm/ka and the emergence of low domes and kopje granitic landforms; these low domes also serve as knickpoints along ephemeral washes. Distant jointing thus plays a key role in generating the bare bedrock surfaces that funnel limited precipitation to bedrock margins — enhancing the canopy cover of perennial plants next to the bare bedrock. Joint-influenced geomorphic processes at Pima Wash generate four distinct process domains: (PD1) armored drainage divides; (PD2) slopes with different granite landforms; (PD3) mid- and upper basin channels that mix knickzones, strath floodplains, and sandy alluvial sections; and (PD4) the main ephemeral channel transitioning to the piedmont. Distant jointing promotes bedrock exposure and rock armoring along drainage divides in PD1 that then concentrates runoff and promotes perennial plant growth. More distant joint spacing on slopes in PD2 promotes exposure of granitic bedrock forms that shed overland flow to their margin and promotes flora and fauna growths along the margins of low granitic domes and kopjes. Similarly, wider joint spacing along ephemeral washes in PD3 leads to knickpoints, which in turn act to concentrate moisture immediately downstream. The stream terraces in PD4 influence the ecology through xeric desert pavements on terrace treads and roofs for coyotes (*Canis latrans*) and gray fox (*Urocyon Cinereoargenteus*) dens on terrace scarps via stage 3 pedogenic carbonate. These four process domains occur in six other randomly selected granitic watersheds with drainage areas <5 km^2 in the Mojave and Sonoran Deserts. Results on rates of geomorphic processes in the Pima Wash watershed provide new insight in the desert geomorphology of small granitic watersheds. Catchment-wide denudation rates (CWDRs) recorded by ^{10}Be sampled along the main ephemeral wash vary between 15 and 23 mm/ka and do not appear to be influenced by knickpoint or knickzone occurrence; instead slightly lower CWDRs appear to be associated with sediment contributions by subbasins with more abundance of bare bedrock forms. Resampling for CWDR after a 500-year flood event from hurricane moisture at two sites along the main ephemeral channel revealed no detectable changes; this finding confirms the average representativeness of CWDR as a long-term denudation proxy and also means that sediment transport on these arid granitic hillslopes must be incremental and without rapid *crest to wash* transport. The first reported measurements of incision rates into a small granitic Sonoran Desert watershed, using ^{10}Be and VML, reveal rates on the order of 70–180 mm/ka in the lower quarter of Pima Wash for the last 60 ka — producing a narrow and deep trench. As this base-level fall propagates upstream, erosion focuses on weaker material with higher joint densities; this facilitates the emergence of domes and kopje landforms with more widely spaced jointing.

1. Introduction

Geomorphic processes alter ecosystem dynamics in different ways that influence where plants colonize, disturbance, and subsequent

* Corresponding author at: Department of Geography Education, Korea University, Seoul 136-701, Republic of Korea.
E-mail address: ybseong@korea.ac.kr (Y.B. Seong).

http://dx.doi.org/10.1016/j.geomorph.2015.12.014
0169-555X/

recovery. Process domains (Montgomery, 1999) work well to better articulate geomorphology and ecosystem dynamics in the Pacific Northwest (Brardinoni and Hassan, 2006; Collins and Montgomery, 2011), in southeastern North America (Troia et al., 2015), in Michigan (Neeson et al., 2012), and in different settings within the Rocky Mountains (Wohl, 2010, 2011; Polvi et al., 2011; Bellmore and Baxter, 2014; Livers and Wohl, 2015). As originally presented, Montgomery (1999, p. 402) considers process domains 'predictable areas of a landscape within which distinct suites of geomorphic processes govern physical habitat type, structure and dynamics; the disturbance regimes associated with process domains dictate the template upon which ecosystems develop.' This paper explores whether process domains can be applied usefully to the very different setting of small arid watersheds.

While arid streams display very different characteristics (Graf, 1988; Clapp et al., 2000; Sutfin et al., 2014; Wohl, 2014) from settings traditionally analyzed for process domains, arid channels and surrounding slopes nonetheless play a vital role in fragile arid ecosystems (Jones and Glinski, 1985; Warren and Anderson, 1985; Sandercock et al., 2007; Stromberg et al., 2009a,b). Conceptually, the understanding of different domains of geomorphic processes is considered important in the planning of the restoration of desert river systems (Laub et al., 2015). Practically in drylands, process domains assist in understanding semiarid grassland catchments in the southwestern USA (Cervantes et al., 2014) and biota in mountainous canyons in semiarid Arizona (Wallace et al., 2010). In particular, spatial variability in plant composition and structure can reflect the location of sediment storage in channels as opposed to straths; the location of small springs associated with subsurface storm flow brought to the surface by bedrock; the ability of deep-rooted phreatophytes to survive droughts through funneling of water through bedrock fracture systems; and the role of flood pulses on seed banks (Hupp and Osterkamp, 1996; Stromberg et al., 2008; Stromberg and Katz, 2011; Hamdan, 2012). Thus, the study of process domains in arid drainages could potentially benefit the understanding of ecosystems dynamics.

The vast majority of dryland watersheds are <5 km^2 (Ives, 1965; McGinnies et al., 1968; Schick, 1974; Lekach and Schick, 1983; Baron et al., 1998), explaining this paper's focus on small drainages. Furthermore, past research on small watersheds has generated important insight on such topics as bedload dynamics (Lekach and Schick, 1983; Hassan, 1990; Reid et al., 1995), hydrologic responses (Yair and Kossovsky, 2002), and sediment budgets (Schick and Lekach, 1993). Because different rock types in arid regions have been shown to alter arid geomorphic processes (Derbyshire, 1976; Mabbutt, 1977; Büdel, 1982; Twidale, 1982; Young and Young, 1992; Gutierrez, 2005), we constrain our focus to small arid watersheds containing only granitic lithologies because granite is studied extensively in arid lands and is also associated with classic arid landforms (Cooke and Warren, 1973; Mabbutt, 1977; Twidale, 1982).

This paper starts by presenting a conceptual model of process domains observed in small granitic watersheds in the Sonoran and Mojave Deserts. We then evaluate the hypothesized domains in a case study at Pima Wash in South Mountain, Phoenix, in the Sonoran Desert, where we analyze rates of geomorphic processes and their effect on desert biota.

2. A process domain hypothesis for small arid granitic watersheds

Fig. 1 presents our working hypothesis of four process domains (PD) found in small arid granitic drainage basins <5 km^2: (PD1) armored drainage divides; (PD2) slopes mixing different granite landforms; (PD3) mid- and upper basin channels that mix knickzones, strath floodplains and sandy alluvial sections; and (PD4) the main ephemeral channel transitioning to the piedmont.

This hypothesis was developed through field observations and interpretation of landforms and associated biogeography in six randomly sampled watersheds in the Mojave and Sonoran Deserts. The process used to select drainages for study first limited the selection to granitic terrains in the Mojave and Sonoran Deserts with drainages <5 km^2 using GIS. A numbered grid superimposed on these areas facilitated random selection of six watersheds:

34.500463°–117.053867° about 3 km^2 in the Mojave Desert
34.676471°–117.000163° about 0.3 km^2 in the Mojave Desert
33.812974°–115.837874° about 1 km^2 in the Mojave Desert
33.001348°–111.678850° about 0.3 km^2 in the Sonoran Desert
33.628765°–112.518101° about 1.6 km^2 in the Sonoran Desert
33.843176°–113.247740° about 1.3 km^2 in the Sonoran Desert.

The construction of Fig. 1 was also informed by prior work on process domains (Montgomery, 1999; Brardinoni and Hassan, 2006; Wohl, 2010; Collins and Montgomery, 2011; Bellmore and Baxter, 2014), prior literature on granitic slopes (Wahrhaftig, 1965; Twidale, 1982; Abrahams et al., 1985; Parsons and Abrahams, 1987; Parsons et al., 2009; Jessup et al., 2011), in combination with a classification of ephemeral streams used to understand mountainous terrain in southwestern Arizona (Sutfin et al., 2014).

The interplay between geomorphic processes and ecosystem characteristics remains the key in the thinking behind Fig. 1. Unlike other process domain studies where events like avalanches and debris flows on slopes offer regular disturbance to the biogeography (Montgomery, 1999; Brardinoni and Hassan, 2006; Wohl, 2010; Collins and Montgomery, 2011; Bellmore and Baxter, 2014), the ecosystem importance of geomorphic processes in small granitic watersheds rests in creating an irregular distribution of water availability in various slope positions and different locations along ephemeral channels (Alcock, 1984; Stromberg et al., 2009a; Stromberg and Katz, 2011). A need that drives this research rests in developing a better understanding of rates of geomorphic processes in small arid granitic watersheds and the connection between geomorphic process domains associated with biota found in these watersheds (Jones and Glinski, 1985; Warren and Anderson, 1985; Sandercock et al., 2007; Stromberg et al., 2009a,b).

3. Pima Wash field area

This study centers on Pima Wash in the South Mountain metamorphic core complex rising in Phoenix, Arizona (Fig. 2). A near-uniform granitic lithology (Reynolds, 1985) underlies the entire Pima Wash drainage basin. The elongated form of the Pima Wash drainage basin developed as the range's relief increased along low-angle detachment faults (Spencer, 2000). Detachment faulting started ~22–20 Ma, and South Mountains underwent arching and unroofing around 20–17 Ma. Uplift and the growth of Pima Wash continued until the region became tectonically quiescent at 14–10 Ma (Fitzgerald et al., 1993; Foster et al., 1993).

Pima Wash contains the basic ephemeral channel morphologies studied elsewhere in the Sonoran Desert (Sutfin et al., 2014). Pima Wash hosts bedrock channels in the upper interior of the drainage that transitions to bedrock mixed with alluvium and ultimately to incised alluvium in an embayment that merges into an alluvial fan piedmont. Although no classic bornhardts emerge in the Pima watershed, bedrock granite forms with wide joint spacing are ubiquitous, including low domes and kopjes created by dome spalling (Fig. 3). Knickpoints and strath floodplains occur where Pima Wash encounters these dome forms. Knickpoints <10 m in height populate the mid- to upstream areas. Strath terraces (Larson and Dorn, 2014) occur in the middle section of the watershed, whereas fill terraces occur only in the downstream reach where the drainage merges into an alluvial fan. The slopes flanking Pima Wash contain a mix of detachment-limited granitic bedrock and grus slopes where grain transport occurs through overland flow associated with rain intensities >36 mm/h (Dorn, 2015).

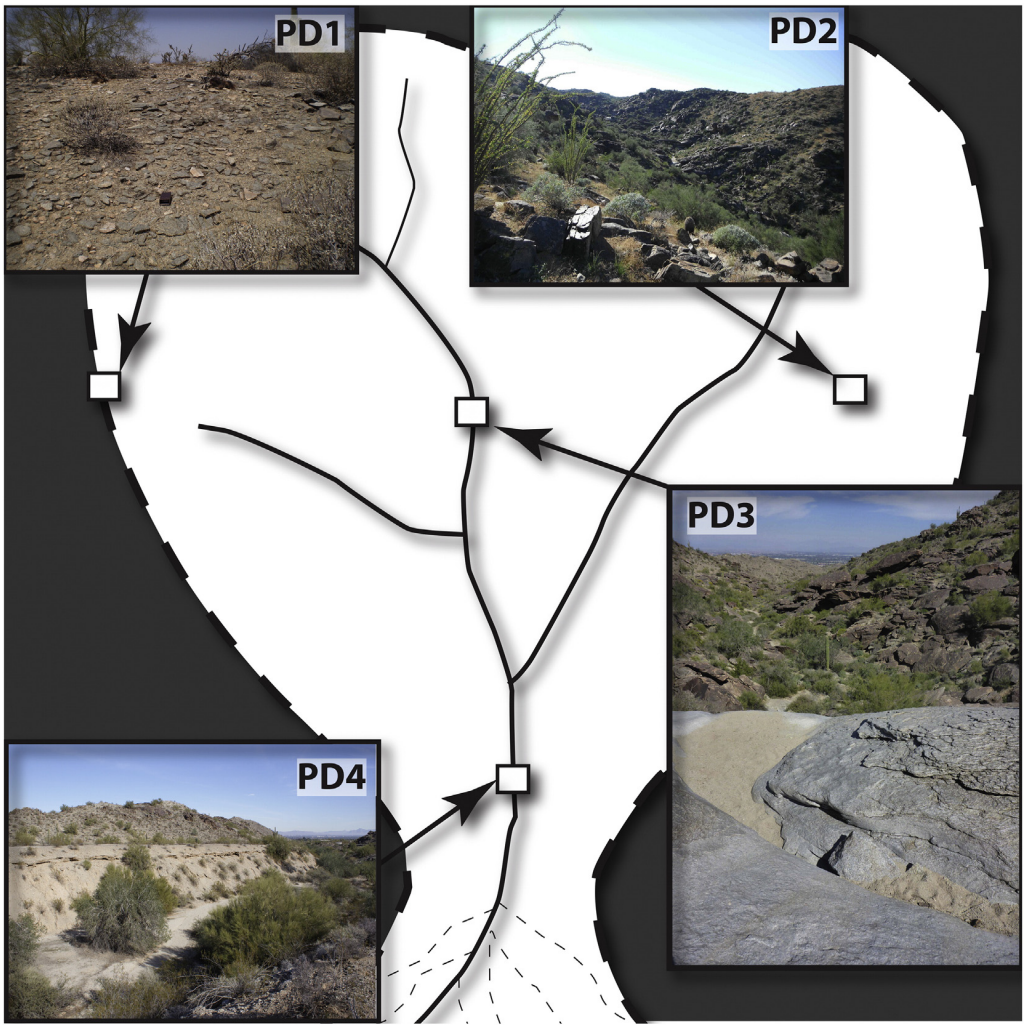

Fig. 1. Process domain hypothesis for small granitic watersheds with drainages <5 km^2 in the Sonoran Desert, in this case illustrated with images from the Pima Wash, AZ, study area. Working downslope from the drainage divide, we propose four process domains: (PD1) drainage divides where cobbles and small boulders armor slopes; (PD2) slopes between the drainage divides and ephemeral channels display a mixture of related but different granite landforms (Twidale, 1982) ordered here by size from large to small: domes; low domes; castle koppie created by spalling of domes; nubbins; tors of various sizes; individual core stones; and areas of mostly grus. (PD3) channels of the Pima Wash and tributaries mix strath floodplains, and knickzones where the ephemeral stream encounters less jointed bedrock and sandy alluvial sections between; and (PD4) the incised main ephemeral channel near the piedmont increasingly mixes progressively more alluvium with bedrock in a downstream direction, flanked by strath terraces that transition to fill terraces in the piedmont embayment.

The present day climate and vegetation of South Mountain resembles much of the rest of the Sonoran Desert in Central Arizona. Annual precipitation displays a bimodal distribution with summer and winter maxima. Summer convective thunderstorms occur during the July–September Mexican Monsoon generated by moist air masses from the gulfs of Mexico and California. Winter frontal rainfall derives from Pacific cyclones. Mean annual precipitation tends to be evenly split between winter and summer, averaging about 200 mm/yr. The arid climate at South Mountain is typified by a distinct biogeography typical of the Sonoran Desert. Representative vegetation like palo verde (*Parkinsonia microphylla*), ironwood (*Olneya tesota*), and elephant trees (*Bursera microphylla*) are common. Additionally, desert scrub vegetation such as creosote bush (*Larrea tridentata*), brittlebush (*Encelia farinosa*), triangle-leaf bursage (*Ambrosia deltoidea*), catclaw acacia (*Acacia greggii*), desert globe mallow (*Sphaeralcia ambigua*), and ocotillo (*Fouquieria splendens*) and succulents such as saguaro (*Carnegiea gigantea*), barrel (*Ferocactus cylindraceus*), and hedgehog (*Echniocereus engelmannii*) cacti are abundant throughout the landscape.

4. Methods

We employed a variety of methods to better understand rates of geomorphic activity as a way to evaluate the ecological importance of different geomorphic process domains.

4.1. Biotic assessments

To assess potential connections among jointing, morphogenesis, and biogeography, we used the line-intercept method, previously established as a reliable technique to gather data on the cover of desert perennial vegetation (Etchberer and Krausman, 1997). In addition to these transect studies, we obtained information from park rangers on patterns of animal occupancy in the different process domains. Line-intercept locations are identified in a supplemental Google Earth file (supplemental KMZ file and explanatory file).

In process domain PD1, we collected line-intercept data from 28 hill-crest sites studied previously in terms of sediment generated by rainfall

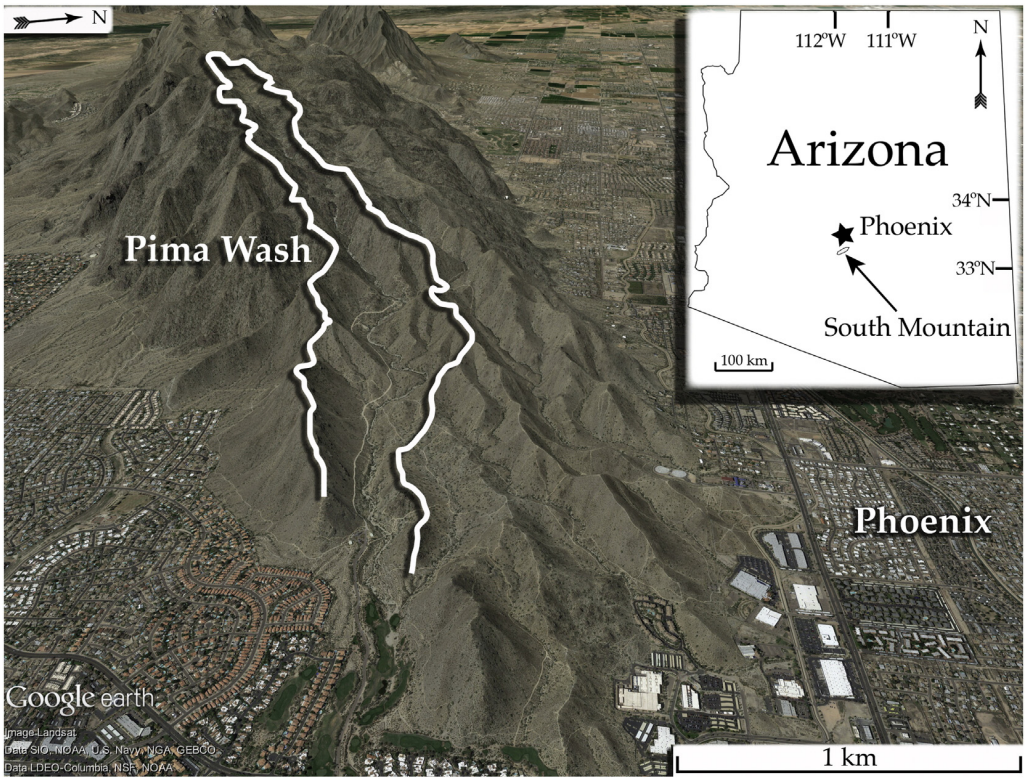

Fig. 2. Simplified west-looking Google Earth view, placing the ~4 km^2 area of Pima Wash drainage in the context of the eastern half of the range in the area of Tertiary granitic rocks. The city of Phoenix surrounds the range.

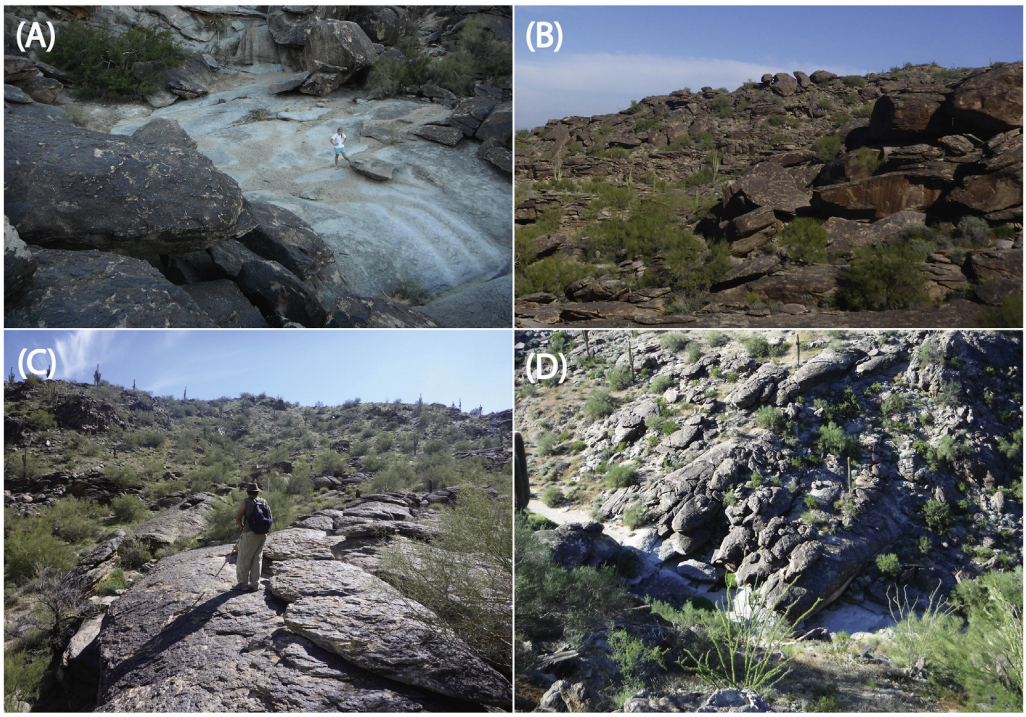

Fig. 3. Typical bedrock forms seen in the Pima Wash watershed consist of low domes (images A and C) and kopje forms produced by spalling of low domes (images B and D). Approximately 8–10-m tall Saguaro cacti provide scale for the kopje forms, while ~2-m tall assistants provide scale for the low domes.

events (Dorn, 2015). In addition to vegetation data on perennial plants, we concomitantly collected data on percent of exposed rock.

In process domain PD2, at randomly sampled hillslope positions studied for joint spacing, four parallel 50-m-long line transects were separated by 10 m, allowing an estimate of plant cover in a 40 m × 50 m box around randomly selected hillslope positions explained in the next section.

In process domain PD3, transect sites were located using the following steps. All knickpoints of the Pima Wash and its tributaries were assigned random numbers with the four highest numbers selected for study. Vegetation transects ranging in length from 120 to 240 m started from the top of each knickpoint and ended at the start of the next lower knickpoint. We measured the percent canopy cover of all perennial trees and shrubs across the full width of the floodplains after subdividing each transect into 10-m segments. For each 10-m segment, three transects were laid out perpendicular to the channel across the floodplain, using the line-intercept method (Etchberer and Krausman, 1997). The first transect was laid out across the floodplain at a 10-m increment, the second of the three transects were laid out 3 m downstream, and the third 3 m more downstream. Data from the three transects were compiled to report an aggregate percent of canopy cover for each of the 10-m segments.

In process domain PD4, four transects of perennial shrub and perennial tree cover were placed perpendicular to the main channel of Pima Wash. The transects also included adjacent landforms, either bedrock slopes with a layer of colluvium <0.5 m thick or the high (T2) stream terrace. Transect locations were not selected randomly. Instead, we placed the transect across areas experiencing the least amount of anthropogenic disturbance of the landscape and the vegetation. Trails and other outdoor recreational activities tend to heavily disturb the landscape in places because Pima Wash resides in a large municipal park. The percent perennial canopy cover was compiled in 10-m sections.

4.2. Comparing jointing to surface stability metrics

In order to better understand the connection between rock jointing and the geomorphic stability of surfaces in Pima Wash, we randomly selected 30 locations for a 3 × 3 m box plot on alternating sides of Pima Wash. After subdividing the slopes of Pima Wash into 30 rectangular areas, alternating east and then west slopes were then subdivided into 10 grids. A random number generator identified a grid, and the center of the grid became the sampling locale. In several cases, measuring jointing or analyzing the weathering grade of bedrock was not possible where a randomly sampled square contained no exposed bedrock. In these circumstances, we used the nearest exposed bedrock to gather joint spacing and weathering grade data. Moving the random sampling location to the nearest exposed bedrock does not exert a bias because that location is still random in its selection. Sampling locations are identified in a supplemental Google Earth file (supplemental KMZ file and explanatory file).

We selected the area method (Wu and Pollard, 1995) from a variety of ways of studying jointing to obtain a quantitative value that can be compared among different locales. The area method defines spacing (S) as

$$S = \frac{A}{1_0 + \sum_{i=1}^{n} 1_i} \tag{1}$$

where l_0 is the side length of a measuring region (3 m in this case), l_i is the total length of fracture in that square, and A ($=l_0^2$) is the area of the square (9 m^2 in this case). Thus, greater joint density generates a lower spacing, reported in millimeters in this study.

We also employed a rock material classification to provide an ordinal ranking of the weathering grade of the material in the randomly selected locale (Ehlen, 1999) of: fresh (F), slightly weathered (S), moderately weathered (M), highly weathered (H), and completely weathered (C).

To assess the hypothesis that closely spaced joints promote surface instability, we employed VML analysis where the method of sampling, sample preparation, and method of estimating age by comparison with published calibrations are presented in detail in the VML literature (Liu, 2003; Liu and Broecker, 2007, 2013). The VML ages are used in this context to provide an estimate for the time of last spalling of the rock surface at the center of each locale. If only grus occurred at the center of a sampled square, the nearest hard-rock surface was sampled for VML — no matter whether it was a cobble, boulder, or bedrock. Each VML age was obtained from a sample of rock a few millimeters across. Certainly, each VML age does not address the overall stability of the entire 3 × 3 m sample region, but it does provide insight into the stability of one randomly selected location.

In order to better understand the process of grus detachment from bedrock surfaces, we also analyzed the degree of attachment between mineral grains on the surface of bedrock and the minerals directly underneath. Field-based strategies to analyze granitic decay remain flawed because moisture can greatly impact the physical strength of grus (Wakatsuki et al., 2007), therefore we employed in situ observations of the grain-to-grain contact.

The samples for grain attachment were obtained from the same locations as the above VML measurements. However, instead of focusing on the microsite appropriate for the VML technique (Liu, 2003), a centimeter–diameter sample was collected from the very center of the clast chipped from the bedrock surface. We then used a scanning electron microscope to image a polished cross-section made normal to the rock surface. Using the digital image processing method to measure porosity (Dorn, 1995; Gordon and Brady, 2002), we measured the percentage of each grain perimeter that was still physically attached to surrounding minerals as viewed in the cross-section (Fig. 4). We acknowledge a problem with this approach — grains that appear to be almost completely detached in one cross-sectional view could still be well attached in the third dimension. Still, by analyzing the cross-section attachments of the first 30 grains viewed, we obtained a metric of the resistance of granitic rock to grus detachment.

4.3. Topographic characteristics

Topographical characteristics reflect the geomorphic processes that in turn link to ecological systems (Montgomery, 1999; Polvi et al., 2011). We obtained topographic data from the Maricopa County Flood Control district with 1.22-m (4-ft) contour intervals. A digital elevation model (DEM) with a resolution of 0.61 by 0.61 m in the horizontal was first constructed from the contour map using ArcGIS. Slope and relief generation employed a moving window of a 3.1-m diameter circle. ArcGIS stream profiler constructed the longitudinal profile, and channel steepness was calculated based on the relationship between area and slope (Flint, 1974; Eq. (2)) using MATLAB scripts (Whipple et al., 2007) and ArcGIS.

$$S = K_s \cdot A^{-\theta} \tag{2}$$

where S is slope, K_s is a channel steepness index, A is area, and θ is a concavity index. The confinement ratio (Polvi et al., 2011) or the degree to which a channel is constricted was calculated from the DEM using the width of the active channel for valley, which is observed during field surveys (Eq. (3)).

$$\mathrm{C} = \text{valley width}/\text{active channel width} \tag{3}$$

4.4. Knickpoints as low emergent granitic domes

Two different strategies were performed to test a hypothesis of the influence of jointing on rates of morphogenesis of exposed bedrock

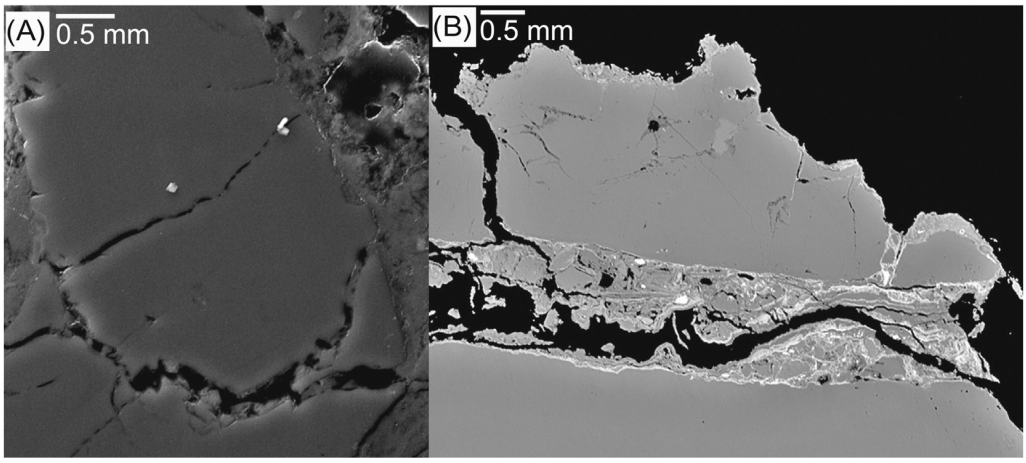

Fig. 4. Electron micrographs of (A) an albite and (B) and orthoclase grain in the process of detachment. While the albite grain remains attached along 62% of its perimeter, the orthoclase grain and linked mineral matter is attached in only 4% of the perimeter.

granite at Pima Wash. Granitic domes with the most distant joint spacing serve as knickpoints along Pima Wash. Thus, Vernier calipers were used to measure erosion at knickpoint flutes annually for 25 years. Second, we collected samples for ^{10}Be concentration at a representative low granitic dome that also serves as a knickpoint.

Vernier calipers were used to measure the erosion of flutes on every knickpoint >0.5 m (Fig. 5). The deepest flutes at 32 knickpoints were measured annually. In making these annual measurements, we assume that surfaces with rock varnish or calcium oxalate rock coatings act as stable ground control points that did not experience any erosion during the 25-year study period; an assumption supported by prior research indicating fluvial abrasion removes these rock coatings (Dorn, 1998). From these ground control points, Vernier calipers measured the position of the deepest flute with a precision of ±0.1 mm. The straths that occur upstream of the measured flutes are homogeneous in granitic lithology (Larson and Dorn, 2014), and the joint spacing (S) of these straths was measured for a distance of 3 m along the full width of the strath.

We also sampled a representative low granite dome in the major knickzone of Pima Wash for ^{10}Be surface exposure dating (Fig. 6). We collected two types of samples: (i) that yield surface exposure ages of the dome (samples 71R, 74R in Fig. 6); and (ii) that are being abraded by storm events that wash over this 7-m knickpoint (samples 72R, 73R). These sampling locations are identified in a supplemental Google Earth file (supplemental KMZ file and explanatory file).

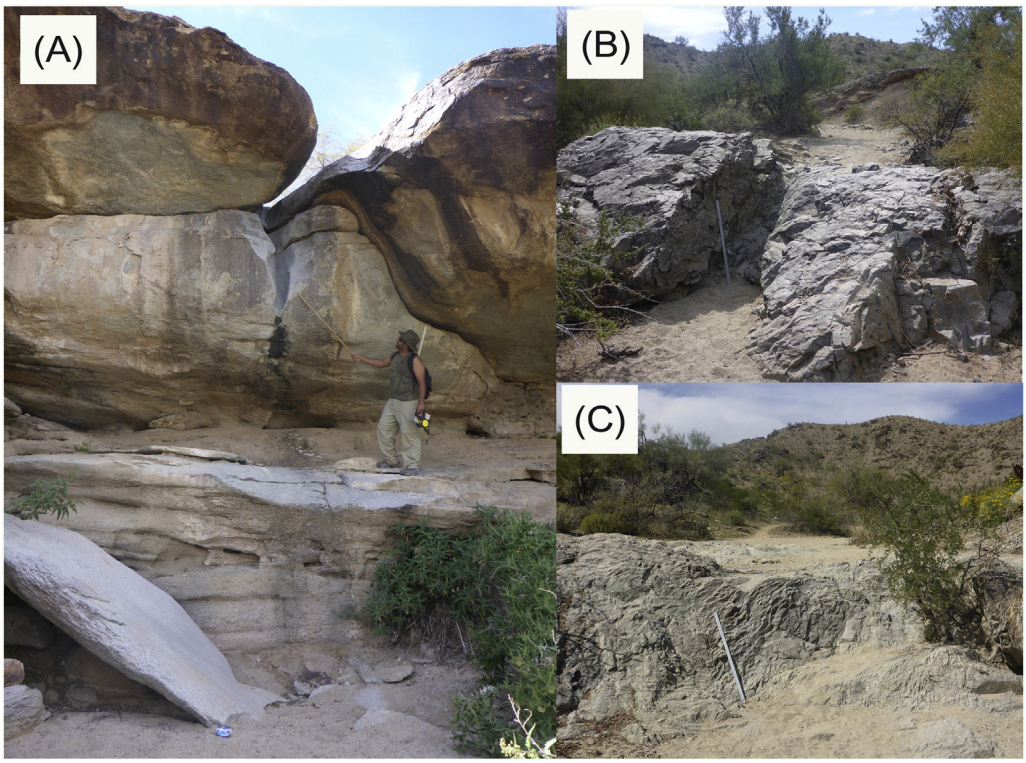

Fig. 5. Vernier calipers using adjacent stable surfaces as ground control points measured any changes to the deepest flutes at Pima Wash knickpoints with an elevation jump of more than 0.5 m. Image (A) shows one of the deepest flutes, while images (B) and (C) show more typical shallow flutes.

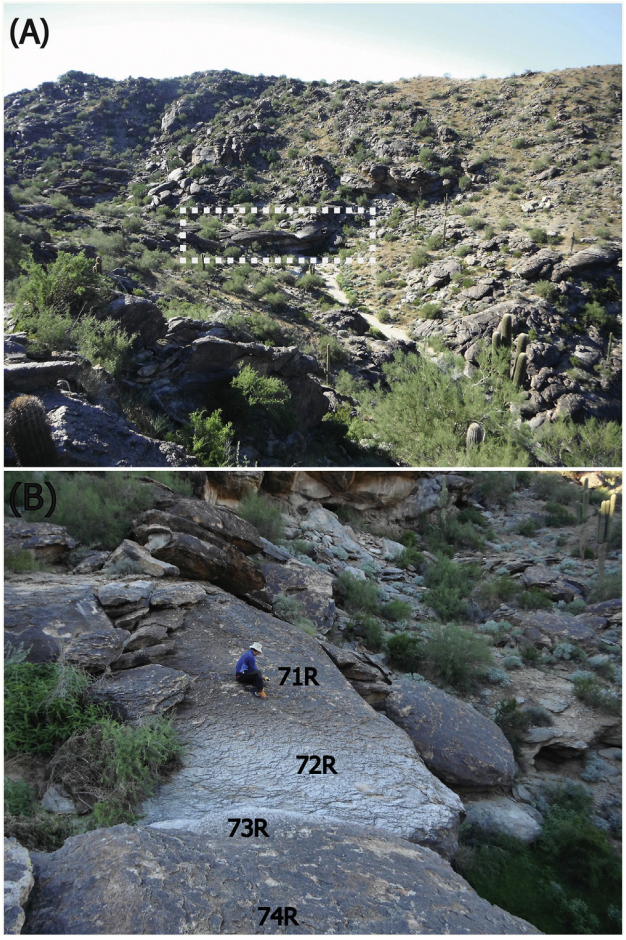

Fig. 6. Surface exposure dating samples (71R–74R) from a 7-m-high knickpoint facilitate a comparison of ^{10}Be surface exposure ages for the surface of a bedrock granite dome (71R; 74R) and also bedrock surfaces experiencing erosion at the knickpoint (72R, 73R). Image (A) looks northwest and identifies the knickpoint in a dotted box where the relief from knickpoint to the ridge crest is ~54 m, while (B) looks northeast.

4.5. Catchment-wide denudation rate

We determined denudation rates from analyses of ^{10}Be content of quartz from Pima Wash alluvium at different locations, where the upstream drainages displayed varying amounts of detachment-limited bare bedrock with widely spaced joints. Catchment-wide denudation rate (CWDR) calculations require a series of basic assumptions (von Blanckenburg, 2005) that are met at Pima Wash: (i) the basin surface has been at steady-state in terms of the nuclide under evaluation where production equals removal from the surface and transport down the wash; (ii) the bulk collection of grains represents a mixture from various basin sources during transport; (iii) landslides with depths >2 m do not occur on slopes of the analyzed basin; (iv) sediment sinks such as fill terraces or alluvial fans do not occur upstream of sampling sites; (v) the basic notion holds true that more ^{10}Be accumulation occurs on slopes that erode slower; and (vi) CWDR measured from a single bulk sample for ^{10}Be content is best interpreted as a maximum value, but that the CWDR is best considered an effective rate if conditions 2 through 4 are satisfied. In the study area, deep-seated landslides do not occur, and thick (>2-m) sediment sinks such as fill terraces, alluvial fans occur only at the bottom of the watershed.

A total of nine samples were collected along the Pima Wash. Sampling locations are identified in a supplemental Google Earth file (supplemental KMZ file and explanatory file). All samples were chemically treated following a standard method (Kohl and Nishiizumi, 1992) at the Cosmogenic Laboratory of Korea University, Seoul, Korea and measured by 6 MV Accelerator Mass Spectrometry (AMS) at the Korea Institute of Science and Technology (KIST), Seoul, Korea (Kim et al., 2016). Isotope ratios were normalized to the ^{10}Be standards (Nishiizumi et al., 2007) using a ^{10}Be half-life of 1.387 ($\pm$0.03) $\times$ 10^6 yr (Chmeleff et al., 2010; Korschinek et al., 2010). Measured ratios are then converted into an absolute ratio of ^{10}Be/^{9}Be in quartz. We calculated the catchment-wide production rate by integrating shielding conditions, latitude–altitude production rate functions (Lal, 1991; Stone, 2000; Heisinger et al., 2002a, 2002b) applying 4.49 $\pm$ 0.39 g^{-1} y^{-1} at SLHL (sea-level, high-latitude) for the ^{10}Be reference spallation production rate in this study (Stone, 2000; Balco et al., 2008). Then for quantifying CWDR, we used the following equation (Lal, 1991):

$$\varepsilon = (P_0/C - \lambda) \cdot z^* \quad (4)$$

where ε means catchment-wide denudation rate, P_0 (atoms g^{-1} yr^{-1}) is ^{10}Be production rate averaged for the sediment source basin, C (atoms g^{-1}) is measured ^{10}Be concentration, λ (y^{-1}) is the decay constant of ^{10}Be, and z^* is Λ/ρ, a depth scale of absorption mean free path where Λ (160 g cm^{-2}) is absorption mean free path and ρ (2.7 g cm^{-3}) is the density of bedrock.

4.6. Stream terrace mapping and estimating Pima Wash incision rate

Sutfin et al. (2014) identified as typical for the Sonoran Desert an ephemeral channel type of incised alluvium at an embayment that transitions to an alluvial fan piedmont. Pima Wash displays this same transition. At Pima Wash, fill terrace treads transition to strath terrace treads higher up in the drainage basin (Larson and Dorn, 2014). Thus, to obtain an insight into rates of incision into strath and fill terraces, these terraces were first mapped and correlated by basic field observations and by analysis of spatiotopographic data collected with a Trimble GeoXH differentially corrected global positioning unit (dGPS). The dGPS resolutions were post processed to produce subhalf-meter accuracy.

Age estimates of three samples were obtained using in situ ^{10}Be analyses for the low strath terrace (T1) and high strath terrace (T2) positions. We also used the varnish microlamination technique (Liu, 2003) and calibration (Liu and Broecker, 2007, 2013) to obtain an estimate for exposure of an intermediate position. Centimeter-resolution surveying measured differences in elevation between positions sampled for ^{10}Be and VML dating: (i) between the highest T2 terrace and a subadjacent eroded bedrock surface sampled for VML; (ii) between the T2 surface and the subadjacent T1 surface; and (iii) between the T1 surface and the modern channel. These sampling locations are identified in a supplemental Google Earth file (supplemental KMZ file and explanatory file).

5. Results

5.1. Biotic observations in different process domains

Cobbles, boulders, and bedrock all armor ridgecrests in process domain PD1 (Fig. 1). The abundance of perennial shrubs such as creosote bush (*L. tridentata*), brittlebush (*E. farinosa*) triangle-leaf bursage (*A. deltoidea*), and trees such as palo verde (*P. microphylla*) appear to be influenced by exposed rock. A statistically significant positive linear regression ($p < 0.01$) linking a higher abundance of plant canopy cover to more exposed rock surfaces (Fig. 7) can be explained through direct field observations made during rainstorms at the sampling sites (Dorn, 2015): runoff from bare rock surfaces funnels to the base of shrubs and trees.

Process domain PD2 of slopes (Fig. 1) consists of granitic materials in various stages of decay from the fresh bedrock of low domes to granitic grus. Perennial shrub and perennial tree canopy cover measured in 40 m $\times$ 50 m grids around the randomly selected hillslope positions

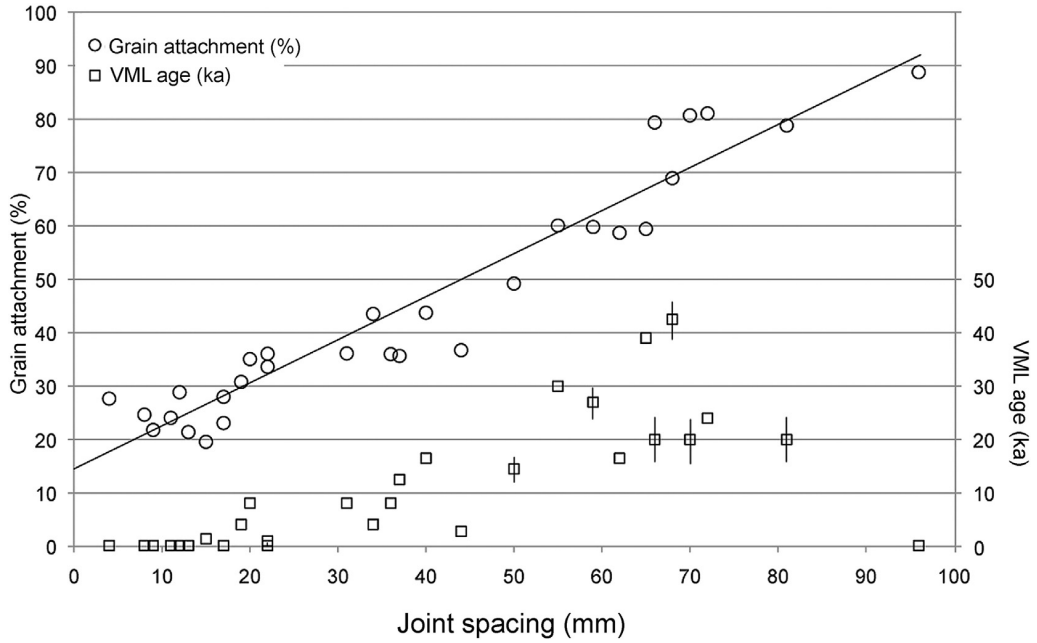

Fig. 7. Linear regression of the percent perennial plant canopy along the ridge crests of Pima Wash studied by Dorn (2015). Three of the 28 sites are not included because of a management decision by South Mountain Park management to remove diseased plants. The correlation is statistically significant at $p < 0.01$ with a Pearson correlation coefficient of 0.553.

(Table 1) shows very different relationships with joint density (Fig. 8). Joint density has no clear influence on perennial shrub cover. In contrast, a statistically significant positive relationship ($p < 0.01$) occurs with perennial trees where more widely spaced joints correlate with more tree cover. Direct field observations during rainstorms reveal that grus-covered slopes in areas of high joint density act as a sieve, except where runoff intensities exceed ~44 mm/h (Dorn, 2015). In contrast, low joint density leads to a greater abundance of bedrock that sheds water to locations where palo verde (*P. microphylla*) and elephant (*B. microphylla*) trees grow.

Table 1
Comparison of joint spacing (Wu and Pollard, 1995), the percent cover of perennial shrubs and succulents; the percent cover of trees; the weathering grade of granite (Ehlen, 1999) to two metrics of geomorphic slope stability: the average and standard deviation of the percentage of a grain surface that is still attached to the underlying mineral; and the last time a rock surface eroded as revealed by its varnish microlamination calibrated age.

Site	Coordinates	Joint spacing (mm)	% cover perennial shrubs & succulents	% cover trees	Weathering grade	% grain attachment (Ave ± SD)	VML age (ka)
1	N 33.34461 W 112.03805	50	11	20	M	49 ± 21	12.5–16.5
2	N 33.34366 W 112.03471	37	10	3	M	36 ± 17	12.5
3	N 33.34662 W 112.03481	40	11	16	M	44 ± 18	16.5
4	N 33.34496 W 112.03217	31	12	5	M–H	36 ± 14	8.1
5	N 33.34634 W 112.03221	4	12	8	H	28 ± 8	<0.3
6	N 33.34650 W 112.02985	8	9	6	H	28 ± 10	<0.3
7	N 33.34892 W 112.02944	11	15	0	H	24 ± 11	<0.3
8	N 33.34779 W 112.02624	66	8	24	S	79 ± 15	16.5–24
9	N 33.35049 W 112.02611	36	11	14	M	36 ± 16	8.1
10	N 33.34980 W 112.02341	81	10	23	S	79 ± 13	16.5–24
11	N 33.35144 W 112.02301	34	13	8	M	44 ± 19	4.1
12	N 33.35064 W 112.02045	96	7	12	S	89 ± 6	<0.3
13	N 33.35243 W 112.02008	13	15	9	H	21 ± 12	<0.3
14	N 33.35117 W 112.01761	55	9	15	S	60 ± 21	30
15	N 33.35389 W 112.01861	62	12	22	M	59 ± 23	16.5
16	N 33.35439 W 112.01771	70	12	17	M	81 ± 13	16.5–24
17	N 33.35611 W 112.01760	9	11	13	H	22 ± 13	<0.3
18	N 33.35478 W 112.01585	68	16	9	S	69 ± 21	39–46
19	N 33.35613 W 112.01527	20	8	9	H	35 ± 18	8.1
20	N 33.35496 W 112.01230	72	8	15	S	81 ± 9	24
21	N 33.35734 W 112.01228	22	9	7	H	34 ± 15	0.9–1.1
22	N 33.35624 W 112.01094	65	14	12	S	59 ± 32	39
23	N 33.35804 W 112.01074	15	8	1	H	20 ± 9	1.4
24	N 33.35708 W 112.00886	44	18	14	M	37 ± 16	2.8
25	N 33.35916 W 112.00928	17	7	0	H	23 ± 12	<0.3
26	N 33.35776 W 112.00732	22	10	16	M–H	36 ± 17	<0.3
27	N 33.36016 W 112.00744	12	12	0	H	29 ± 16	<0.3
28	N 33.35888 W 112.00530	19	12	5	M–H	31 ± 20	4.1
29	N 33.36202 W 112.00398	17	7	0	H	28 ± 13	<0.3
30	N 33.35962 W 112.00389	59	8	7	S	60 ± 22	24–30

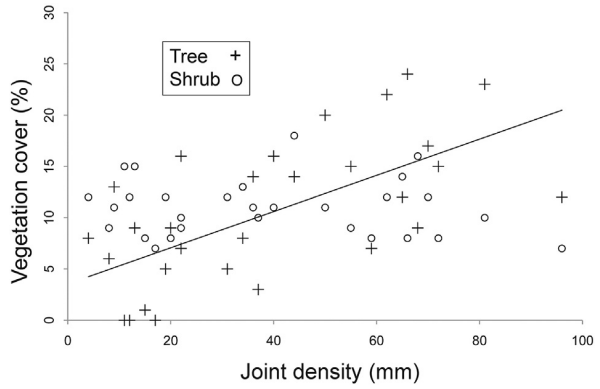

Fig. 8. Scatterplot of percent perennial shrub cover (open circles) and percent tree cover (crosses) compared with joint spacing; data are presented in Table 1. While a linear regression of shrub cover versus joint density had no statistical significance, the linear regression shown here for percent tree cover versus joint density is statistically significant at $p < 0.01$ with a Pearson correlation coefficient of 0.637.

While the general conclusion can be drawn that joint spacing on slopes plays a key role in perennial tree cover in PD2, certain species-specific trends are noteworthy. Elephant tree occupies the widest joint spacing (S > 65 mm) on south-facing slopes. Ocotillo (*F. splendens*) favors moderate joint spacing (S ~ 30–50 mm) on north- and east-facing slopes. Creosote bush (*L. tridentate*) and brittlebush (*E. farinosa*) desert scrub species tend to occupy the closest joint spacings ($S < 20$ mm) irrespective of aspect. Teddy bear cholla (*Cylindropuntia bigelovii*) prefers close joint spacing ($S < 35$ mm) and south-facing slopes.

Process domain PD3 of the channels within the Pima Wash drainage includes strath floodplains, knickpoints (often in knickzones), and sandy alluvial sections between the knickpoints. The four randomly selected knickpoints lack perennial vegetation on the steep bare bedrock surfaces (Fig. 9). The highest density of perennial vegetation, in contrast, occurs immediately beneath the knickpoints with canopy cover exceeding 70% for three of the study areas. Based on field observations of these and other knickpoints during precipitation events, water plunging over the knickpoint into the sandy alluvium facilitates retention of water in the alluvium and plant growth. It is the greater abundance of water, thus, that explains the jump in canopy cover directly beneath knickpoints. As discharge infiltrates into sandy reaches beneath the knickpoint, water availability lessens and a reduction in canopy cover occurs downstream in each of the study areas (Fig. 9A–D).

Process domain PD4 of the incised Pima Wash near the piedmont consists of a low-relief floodplain surrounded by either bedrock slopes mantled by <0.5 m of colluvium or the high T2 stream terrace that transitions from strath (Fig. 10A) to fill (Fig. 10B–D). The greatest canopy cover occurs on the east-facing sides of the wash, explained most simply by afternoon shading and by water shed from adjacent slopes. The least vegetation cover occurs on the desert pavements of the T2 terrace treads.

5.2. Jointing and surface stability metrics

Joint spacing (*S* in Eq. (1)) sampled at 30 randomly selected plots maintains a statistically significant linear relationship with percent mineral grain attachment (Table 1; Fig. 11). Closer joint spacing means lower percentages of grain attachment with a statistically significant ($p < 0.01$) R^2 value of 0.92.

Joint spacing also maintains a clear connection to the stability of surfaces in the randomly selected plots — as measured by when rock varnish last detached using VML. Because VML ages are not normally distributed, a linear regression is not appropriate. Still, the plotted data (Fig. 11) reveal that ongoing surface erosion recorded by young VML ages relates to close joint spacing, where a likely explanation rests in particle detachment *resetting* the varnish VML clock. In contrast, widely spaced joints with better grain attachment foster surface stability reflected by the last erosion event in the mid-Holocene to late Pleistocene.

Because close joint spacing results in grus production and more distant joint spacing results in more stable bedrock surfaces, joint spacing ultimately plays a key role in explaining the perennial plant cover; as noted in Section 5.1 where overland flow shed by the stable bare bedrock creates the pockets of biotic enhancements seen in Figs. 7-10.

5.3. Topographic analyses

The Pima Wash watershed slope map (Fig. 12C) displays an irregular distribution of higher and lower slope angles that are a function of the irregular distribution of granite landforms. Regions of low joint spacing with abundant grus generate lower slope angles. The sides of granite landforms such as the domes observed maintain steep angles, as do the koppie, nubbins, and tors associated with broken-down domes. Relief (Fig. 12D) shows a similar pattern for the same reasons. A knickzone produces the steepest sections of Pima Wash (Fig. 12E and G), where low granite domes produce the larger individual knickpoints within that zone.

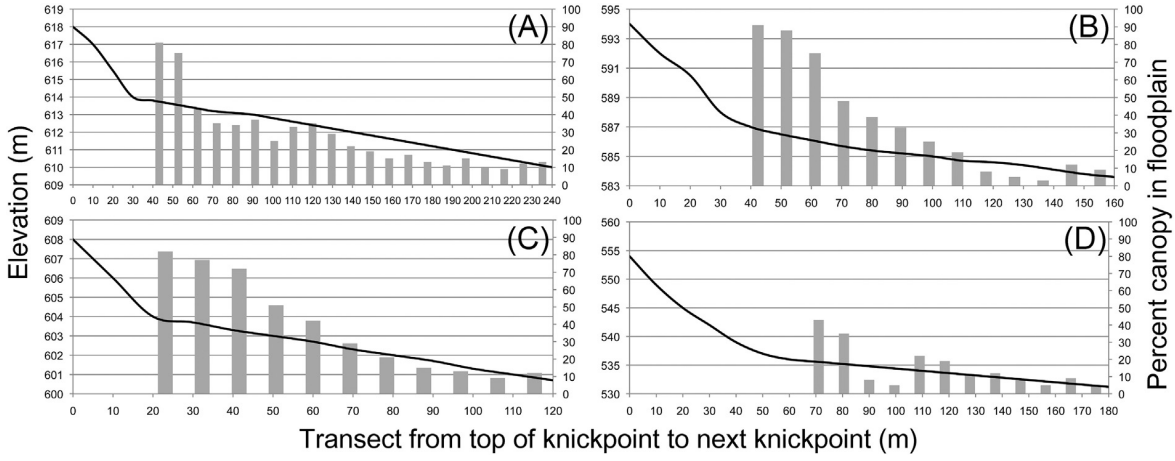

Fig. 9. Vegetation transects across the full width of floodplains downstream from four randomly selected knickpoints, where transects end at the top of the next downstream knickpoint. The canopy of all perennial shrubs and trees are reported as a percentage in 10-m increments. The following coordinates are at the top of the four randomly selected knickpoints: (A) N 33.351801° W 112.019908°; (B) N 33.353061° W 112.017866°; (C) N 33.356725° W 112.020204°; and (D) N 33.356182°W 112.012442°.

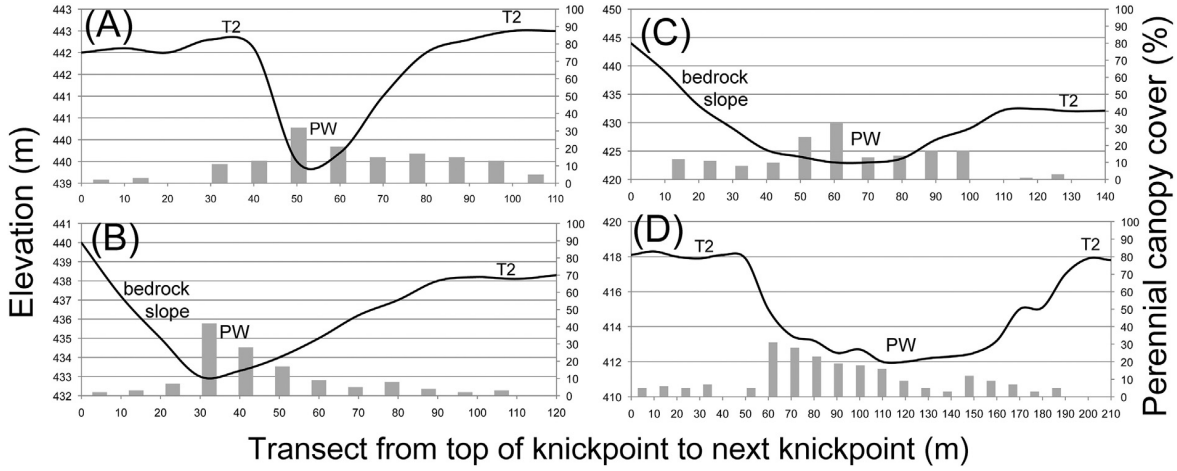

Fig. 10. Vegetation transects across Pima Wash including adjacent bedrock slope and T2 stream terrace landforms. The canopy of all perennial shrubs and trees are reported as a percentage in 10-m increments. The following coordinates are the locations where the transects cross Pima Wash (PW): (A) N 33.361687°W 111.994024°; (B) N 33.361931°W 111.991811°; (C) N 33.362352°W 111.989183°; and (D) N 33.363735°W 111.982849°.

The highest confinement of Pima Wash (Fig. 12F) occurs in association with locations of strath stream terraces that display the greatest joint spacing. Low confinement occurs in association with higher joint spacing in the bedrock exposed within the strath terrace. Direct observations of several flash floods in association with these low and high confinement zones reveal a repeated pattern. As floods squeeze through the constricted areas, eddies form upstream of the confinement. Eddies circulate suspended sediment and flood debris that piles up on the sides of the channels. This finer sediment traps moisture inside the sandy lenses. These sandy and silt lenses provide avenues for the roots to grow along these lenses, and the roots in turn provide structures for animal burrows of the Harris' antelope squirrel (*Ammospermophilus harrisii*). In addition, this flood-moistened alluvium immediately upstream of knickpoints fosters javelina (*Tayassu tajacu*) habitat, where greater phreatophyte cover provides shade, moisture, and loose sand for digging.

5.4. Knickpoints as low emergent granitic domes

Of the 32 knickpoints observed for 25 years, only two experienced measurable erosion (Fig. 5B and C). The knickpoints portrayed in Fig. 5B experienced 1.9 mm of erosion in 25 years, and the knickpoint shown in Fig. 5C experienced 1.4 mm of erosion in 25 years. Thus, little contemporary evidence exists to suggest that the knickpoints experience significant historical erosion. The strath floodplains that occur upstream of these knickpoints have an average and standard deviation joint spacing (S) of 76 ± 18 mm.

The longer-term perspective obtained from in situ ^{10}Be concentration at a representative knickpoint formed by a low dome reveals long-term stability. The apparent exposure ages of this dome range from 89 to 153 ka (Pima 71R, 72R, 73R, and 74R in Table 2). The two positions where the ephemeral channel traverses the low dome (72R and 72R in Fig. 6) are both the most stable (153 ka in the center of the ephemeral channel) and least stable (89 ka on the side of the ephemeral channel). In situ ^{10}Be concentration alternatively provides insight into maximum rates of surface erosion, and the four collection sites on this low dome range from 4.6 to 8.4 mm/ka (Table 2).

The low granitic domes that serve as knickpoints produce a moisture-related effect that promotes phreatophyte growth. Strath floodplains extend several meters upstream of knickpoints and inhibit vegetation growth, but sandy lenses accumulate a bit farther upstream of knickpoints; the bedrock underneath the sand pond water. Saltcedar (*Tamarix chinensis*) grows in the channel in these locations, and saguaro (*Carnegiea gigantea*) grows on rocky slopes immediately adjacent to these subsurface water pools. Pits dug to a depth of 2.5 m through the sandy alluvium reveals that saltcedar roots penetrated bedrock joints beneath the sandy alluvium.

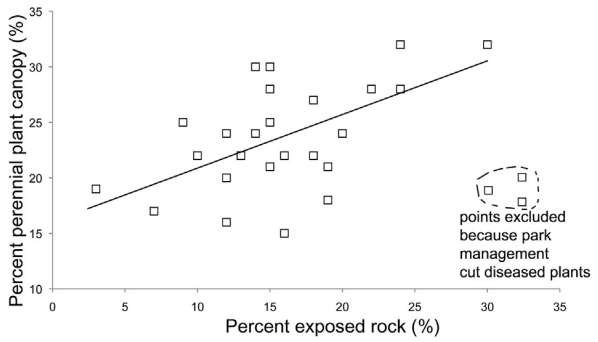

Fig. 11. The relationship between joint spacing (S, in Eq. (1)) and two metrics of surface stability: the percentage of grain attachment (circles) and the VML age that provides a minimum age for the last time the sampled surface spalled (square). The standard deviations of the grain attachment measurements are indicated in Table 1. The line denotes the linear regression of grain attachment percentage (G) = 14.52 + 0.79 S (joint spacing) with Pearson's correlation coefficient of 0.96.

5.5. Catchment-wide denudation rate

Catchment-wide denudation rates (CWDR) for different positions along Pima Wash vary between 15 and 23 mm/ka (Table 2). Taken as a whole, CWDR rates do not vary significantly with position along the longitudinal profile or with position with respect to major knickpoints. Of note, resampling two positions (Pima 55a, 56a) after a 500-year precipitation event on 8 September, 2014 and corresponding flood from hurricane moisture did not alter denudation rates.

5.6. Pima terraces and incision rate

The Pima Wash stream terraces (Fig. 13) consist of small isolated remnants of a lower T1 terrace with two in situ ^{10}Be ages on exposed bedrock of 16.2 ± 1.4 and 21.7 ± 2.0 ka (Table 2). The higher T1 terrace in a strath location yielded a ^{10}Be age of 60.1 ± 2.7 ka (Table 2). Rock varnish collected from a patch of bedrock between the T1 and T2 terraces yielded a VML age between the 39 and 30 ka calibration laminations (Fig. 14). Taken altogether, these data provide rough insight

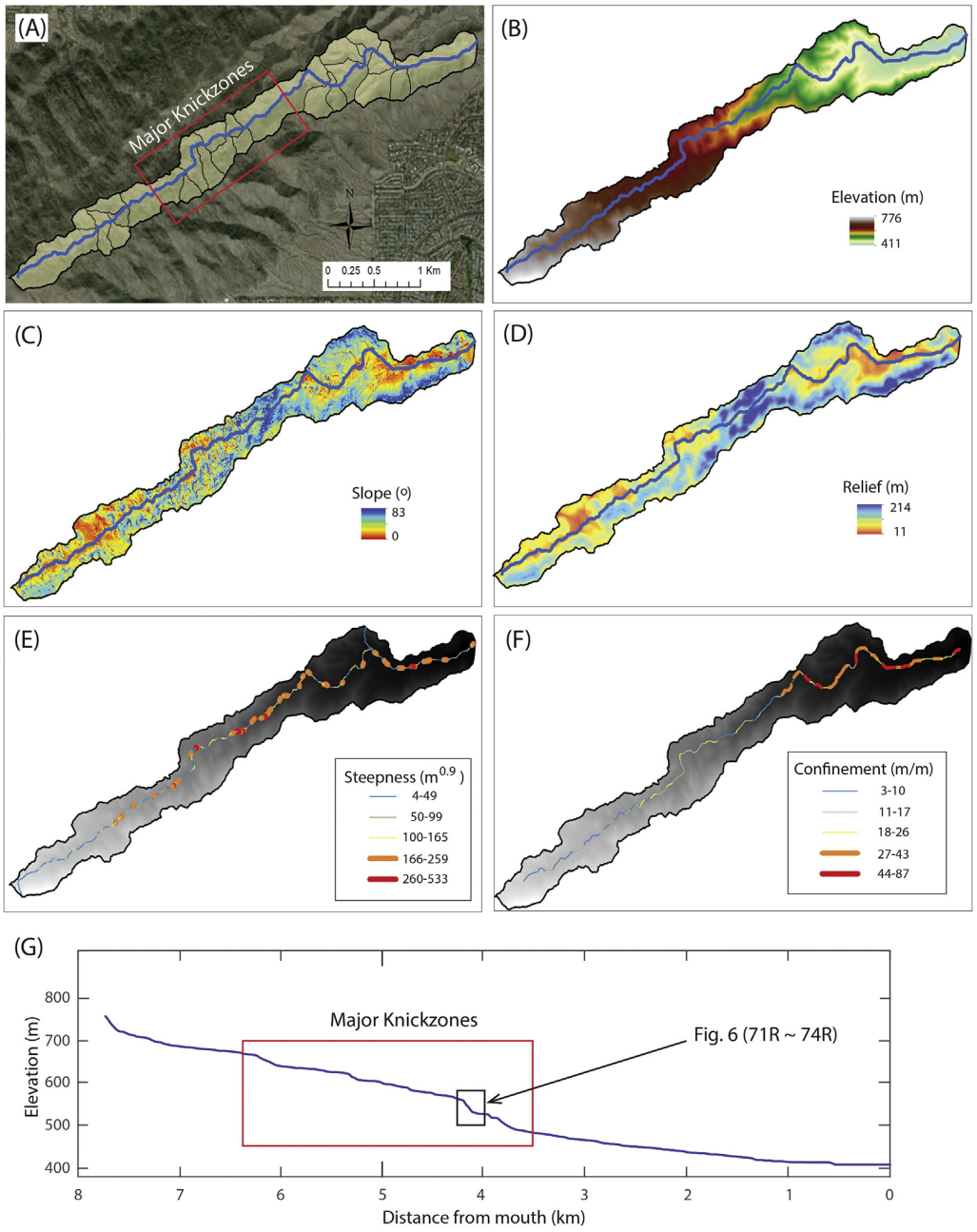

Fig. 12. Topographic characterization of the Pima Wash watershed. (A) Pima Wash with its tributary channels; (B) elevation; (C) slope; (D) relief; (E) steepness index of the wash; (F) confinement ratio of the wash; (G) longitudinal profile.

into rates of incision during the last glacial cycle, being on the order of ~70–180 mm/ka (Fig. 13).

The extensive T2 stream terraces along Pima Wash influences a variety of ecosystem dynamics in addition to the observations presented in Section 5.1. While hillslope runoff flows directly into Pima Wash and tributaries upstream of the major T2 terraces, the terrace treads force this flow into rills and small gullies between the terrace scarp and terrace tread — providing enough moisture for denser scrub and habitats for Gambel's quail (*Callipepla gambeilii*), Bewick's wren (*Thryomanes bewickii*), and black-throated sparrows (*Amphispiza bilineata*).

The T2 terrace morphogenesis influences the location of animal dens. While the top of terrace treads host desert pavements with a greatly reduced vegetation cover dominated by Creosote bush (*L. tridentata*), stage 3 calcrete forms on T2 treds. The petrocalcic horizon provides a secure roof for coyotes (*Canis latrans*) and gray fox (*Urocyon cinereoargenteus*) when they dig out dens underneath the calcrete.

6. Discussion

6.1. Process domains in a small arid granitic watershed

Montgomery (1999) developed the concept of process domains in a humid ecoregion. Our findings from the Pima Wash watershed, Sonoran Desert, reveal process domains (Montgomery, 1999) to be useful in understanding biota in the very different setting of small arid granitic watersheds. Spatial variability in perennial shrub cover and perennial tree cover reflects locations where overland flow is shed from: bare

Table 2
Catchment-wide denudation rate (CWDR) and incision (or surface erosion) rate based on cosmogenic ^{10}Be analyses. The first part of this table presents CWDR data and the second part surface exposure dating results (more detailed locations are shown in supplemental KMZ file).

Sample ID	Latitude (°N)	Longitude (°E)	Elevation (m a.s.l.)	Production rate[a] (atoms g^{-1} yr^{-1})	^{10}Be concentration[b] (10^5 atoms g^{-1})	Denudation rate (mm ka^{-1})	Timescale[c] (ka)
CWDR							
PIMA51	33.362	111.990	422.6	6.239	1.71 ± 0.24	21.90 ± 3.19	27.9 ± 4.0
PIMA52	33.363	111.996	442.4	6.224	1.91 ± 0.25	19.49 ± 1.57	31.3 ± 2.5
PIMA53	33.361	112.004	464.3	6.512	1.70 ± 0.11	23.06 ± 1.53	26.5 ± 1.7
PIMA55	33.360	112.006	471.0	6.546	2.00 ± 0.57	19.62 ± 5.62	31.1 ± 8.9
PIMA55a[d]	33.360	112.006	471.0	6.546	2.07 ± 0.56	19.01 ± 5.21	32.1 ± 8.8
PIMA56	33.356	112.015	568.2	6.679	2.66 ± 0.78	15.00 ± 4.44	40.7 ± 12.0
PIMA56a[d]	33.356	112.015	568.2	6.679	2.59 ± 0.18	15.40 ± 1.85	39.6 ± 2.7
PIMA57	33.351	112.022	624.8	6.799	2.20 ± 0.63	18.54 ± 5.35	32.9 ± 9.5
PIMA58	33.348	112.029	670.0	6.906	1.88 ± 0.47	22.09 ± 5.57	27.6 ± 6.9
Surface dating				^{10}Be concentration	Erosion rate (mm ka^{-1})[e]	Age (ka)[f]	
T2 terrace (P35)	33.362	111.987	418.2	1.15 ± 0.10	39.38 ± 4.58	21.7 ± 2.0	
T2 terrace (P36)	33.362	111.988	419.3	0.85 ± 0.07	53.68 ± 6.13	16.2 ± 1.4	
T1 terrace (P54)	33.361	112.003	469.7	3.28 ± 0.14	12.99 ± 1.12	60.1 ± 2.7	
Dome (P71R)	33.357	112.011	528.7	8.01 ± 0.25	4.89 ± 0.43	144.0 ± 13.7	
Strath (P72R)	33.357	112.011	527.0	8.50 ± 0.15	4.57 ± 0.38	152.6 ± 14.0	
Strath (P73R)	33.357	112.011	527.5	4.96 ± 0.12	8.43 ± 0.68	88.5 ± 8.1	
Dome (P74R)	33.37	112.011	528.5	7.20 ± 0.25	5.56 ± 0.50	128.2 ± 12.4	

[a] Total catchment-wide production rate from spallogenic and muonic production. Reference production rate for SLHL is 4.49 g/yr (Stone, 2000).
[b] Normalized with standard 07KNSTD and corrected for process blank. Error propagation was based on Balco et al. (2008). The large value combines internal and external errors.
[c] Timescale of catchment-wide denudation rate is calculated using Eq. (2) and accounts for the duration over which a depth of $z^*(=\Lambda/\rho \sim 60$ cm) surface in the basin denudes.
[d] Collected in October of 2014 from the same locations of PIMA55 and PIMA56 after a 500-year precipitation event occurred on 8 September of 2014 from hurricane moisture.
[e] Maximum erosion rate assuming steady-state erosion.
[f] Minimum exposure age assuming zero erosion rate.

rock surfaces exposed along ridge crests of process domain PD1 (Fig. 7); granitic bedrock forms associated with widely spaced joints on slopes in process domain PD2 (Fig. 8); and immediately downstream of knickpoints in the channels of process domain PD3 (Fig. 9). The basic finding that enhanced water availability in different geomorphic process domains promotes a statistically significant biotic response is consistent with ecosystem scholarship on the importance of water availability in the Sonoran Desert (Jones and Glinski, 1985; Warren and Anderson, 1985; Sandercock et al., 2007; Stromberg et al., 2009a,b).

The interdisciplinary field of biogeomorphology utilizes a variety of research strategies to explore connections between desert landform processes and ecosystems (Parker, 1991; Wondzell et al., 1996; Parsons et al., 2009; Wainwright, 2009; Michaud et al., 2013). In this prior research, a process domain approach has not been applied previously. Given the prevalence of small, granitic watersheds in the arid environment, assessing the process domain concept in this study helps address a fundamental gap in our understanding of these complex systems.

Four process domains in the study area emerged from observations of geomorphic and biogeographic characteristics (Fig. 1). In PD1 along drainage divides, rock armoring promotes vegetation growth in this xeric setting by funneling runoff to roots of perennial plants (Fig. 7). In PD2, while joint spacing does not appear to influence overall perennial shrub canopy cover on slopes, it does influence trees (Fig. 8). Zones of closer jointing on slopes can sometimes lead to chutes of grus sand, creating xeric habitats on slopes that support *Opuntia bigelovii* on south-facing aspects. Then, where these chutes encounter strath channel bottoms, springs emerge and can last weeks after a rain event. South Mountain Park rangers report that these springs offer habitat for amphibians such as *Bufo alvarius* and insects such as bees and wasps (e.g. *Apis mellifera*, *Diadasia* spp., *Steniolia* sp.).

In PD3, the low domes that also serve as knickpoints shed runoff that fosters the growth of vegetation (Fig. 9). Because erosion rates for this low dome are a third of CWDR of 15–23 mm/ka, we infer that this low dome must be growing in relief over time. Direct field observations during rain events could explain how the dome grows and the surrounding vegetation responds. Bare bedrock sheds water efficiently, and this runoff funnels to rills on the perimeter of the dome — as well as directly to Pima Wash. Water flowing down the rills transports grus to the channel. This process also promotes the growth of phreatophytes such as ironwood (*Olneya tesota*) and elephant trees (*Bursera microphylla*) that obtain additional moisture. In addition, park rangers report that beehives and amphibians occur in greater abundance adjacent to low domes.

As noted, strath floodplains in PD3 typically occur immediately upstream of granitic knickpoints where the valley also widens. This is similar to the description of crystalline bedrock strath in the Poudre River, Colorado, USA (Wohl, 2008). Also, Pima Wash straths are homogeneous (Wohl and Merritt, 2001) in that they are granite with low joint spacing (Wohl, 2008). The distribution of these straths connects geomorphic processes to ecology in several ways. First, strath widening links to enhanced mineral decay associated with vegetation along channel banks (Larson and Dorn, 2014). Second, straths pond moisture inside meter-thick sandy lenses deposited on straths. These lenses retain water after flash flooding (Larson and Dorn, 2014). While flash flooding in general clears the way for the establishment of new plants, the invading *T. chinensis* has been largely unable to establish itself along Pima Wash because of the paucity of post-flooding moisture needed by the plant (Warren and Turner, 1975). The exception has been in these sandy sections immediately upstream of knickpoints. There exists a sufficient supply of water ponded on top of the bedrock to allow the establishment of saltcedar roots. Some of the *T. chinensis* established a sufficient root density to be able to survive the 500-year flash flooding from the 8 September, 2014 hurricane moisture event.

The lack of change in CWDR before and after the 500-year hurricane moisture event suggests that sediment transport processes acting along crests in PD1 and slopes in PD2 do not reach ephemeral washes in PD3. That the CWDR ^{10}Be signal remained the same before and after this major event suggests that arid granite hillslope sediment transport in the Pima drainage occurs in short-distance steps, allowing ^{10}Be to accumulate slowly. Alternatively, the crest and hillslopes where sediments are (very slowly in our study area) detached from the bedrock is weathering-limited, so that they are quickly transported into the channel from which we collected sediment samples for CWDR. The

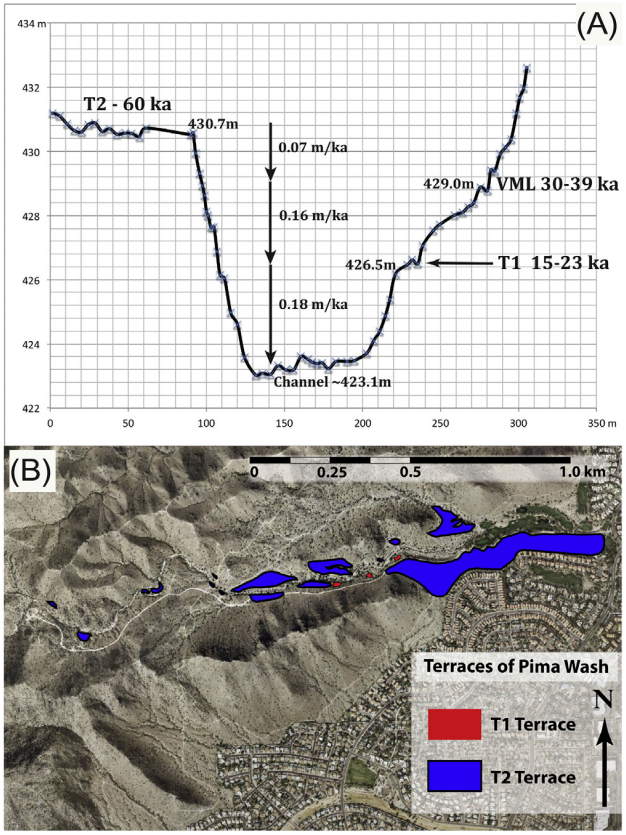

Fig. 13. Small T1 terrace remnants rest inset into more extensive T2 terrace surfaces along the lowest kilometer of Pima Wash. As noted by Sutfin et al. (2014), incised alluvium fill terraces tend to characterize arid basins in the Sonoran Desert and occur close to the piedmont — in this case occupied by the houses. The cross-section identifies positions sampled for ^{10}Be and VML. Taken at face value for the central tendency of these ages, arrows identify rough estimates of incision rates between different positions.

ecosystem implication is that biota on slopes in PD2 do not have to cope with disturbance related to sudden transfers of sediment, such as occurs from avalanches or debris flows.

In PD4, great contrasts exist in moisture availability within the entrenched wash as compared with the T2 terraces on the margin of the wash (Fig. 10). Whereas very little perennial growth occurs on terraces, abundant plant cover occurs in the wash, especially on the east-facing side protected from afternoon solar radiation. Geomorphic processes offer coyotes and foxes roofs for their dens in PD4, specifically the stage 3 calcrete formed underneath surface desert pavements. Coyotes dig out the soft fill of sand underneath the calcrete that then serves as a solid roof for their den. The coyotes hunt both within the South Mountain nature preserve and in the adjacent urban landscape (Grubbs and Krausman, 2009).

A speculative connection between process domains and paleoecological conditions involves the CWDR data (Table 2). Because CWDR measures erosion rates over glacial–interglacial timescales, the link between CWDR and ecosystem dynamics could potentially connect to paleoecology. Although no paleoecology data exists for South Mountains, pollen and packrat midden evidence for the Sonoran Desert and adjacent uplands suggest that the region was cooler and wetter in the latest Pleistocene. Pollen records in northern Baja California remained similar from 44 to 13 ^{14}C ka BP —a combination of pines, junipers, and sagebrush in that area indicating more humid and cooler conditions (Lozano-García and Ortega-Guerrero, 2002). Packrat midden sequences in the Sonoran Desert suggest that dwarf conifer vegetation of *Juniper osteosperma* and *Pinus monophylla* grew in the lower Sonoran Desert with elevations similar to South Mountain in this same late Pleistocene time range (Van Devender, 1990; Allen et al., 1998; McAuliffe and Van Devender, 1998). Thus abundant evidence of a wetter and cooler time generating more extensive vegetation in the last glacial period could have slowed erosion rates by generating more transport-limited sections of hillslopes; this cooler and wetter climate could have aided in the production of grus sampled for CWDR.

The remainder of the discussion section focuses on specific geomorphic implications of the results, while also weaving in connections between specific geomorphic themes and their potential impact on other ecological patterns not discussed in Section 6.1.

6.2. Jointing and surface stability

Abundant geomorphic research recognizes the importance of jointing in landform evolution (Eyles et al., 1997; Scheidegger, 2001; Molnar et al., 2007; Paradise, 2013; St Clair et al., 2015), and this is

Fig. 14. Pima Canyon displays a mix of fill terraces that transitions to an alluvial fan at the mouth of the wash. Approximately 1.8 m underneath the highest surface of the T2 fill terraces, patches of bedrock intermixed with alluvium host rock varnish that started to form soon after incision started. Incision into this terrace exposed bedrock that has a VML signal between WP3 and WP4 or between 39 and 30 ka. WP stands for wet period.

particularly true for morphogenesis in granitic terrain (Linton, 1955; Twidale, 1982; Ehlen, 1992; Migon and Goudie, 2003; Jessup et al., 2011; Becker et al., 2014). Molnar et al. (2007, p.12) postulate that jointing rests at the core of geomorphic weakness: [h]ere we speculate that a corollary to the arguments given above about the role of tectonics as a crusher of rock is that in those places where rock has dodged the rock crusher, it may be stronger and less easily removed by erosive agents. Jointing can be particularly important in arid weathering-limited landscapes where slope processes and form often depend on joint pattern and density (Abrahams et al., 1985; Howard and Selby, 2009; Viles, 2013).

Joint spacing appears to influence the stability of detachment-limited rock surfaces. Closer joint spacing leads to the enhancement of mineral dissolution along grain boundaries; 92% of the variance in grain-to-grain attachment can be explained by joint spacing (Fig. 6). Closer jointing facilitates water transfer that then reduces grain-to-grain attachment, which in turn leads to particle detachment. Surfaces with lower grain attachment experienced much more recent spalling episodes, in the last 300 years, as recorded by VML analyses. Conversely, distant jointing promotes more grain attachment and promotes slower rates of spalling (Fig. 11).

The mixture of areas with more stable bedrock from distant jointing and eroding grus slopes from close jointing leads to a mixture of slope characteristics as seen in Fig. 12C: steep slopes occur on the flanks of bedrock domes, flatter slopes on the top of the domes, and intermediate slopes on eroding grus surface. This observed connection between jointing and slope steepness in arid granitic terrain is not new (Twidale and Bourne, 1975; Twidale, 1982; Howard and Selby, 2009; Parsons et al., 2009). Our research, however, contributes new insight into the importance of mineral grain attachment and rates of bedrock detachment (Fig. 11).

6.3. Denudation rates

The different sampling sites for CWDR along Pima Wash had erosion rates ranging from 15 to 23 mm/ka using ^{10}Be. These rates, surprisingly (Gudmundsdottir et al., 2013; Legrain et al., 2015), do not relate to the distribution of knickpoints and major knickzones along Pima Wash (Fig. 12).

Considering the 1σ error term in Table 2, CWDR rates overlap. Still, if the central tendencies are a valid indicator of lower and higher denudation rates, a recent review could suggest an alternative explanation for the subtle variability in erosion rates — promoting the observation that plants can increase the thickness of weathered material and erosion rates compared with plant-free outcrops (Amundson et al., 2015). This corresponds with our observations. Subbasins with more bedrock forms (e.g., low domes, kopje) supply sediment to Pima Wash CWDR locations with slightly lower erosion rates of 15–20 mm/ka (e.g. Pima 52, 55–57 in Table 2) than basins with fewer bedrock forms and erosion rates of 22–23 mm/ka (e.g. Pima 51, 53, and 58 in Table 2).

In contrast, increases in vegetation cover lower CWDR erosion rates in the Kenya Rift with similar climate and the same granitic lithology from 130 mm/ka on sparsely vegetated slopes to 80 mm/ka on more densely vegetated slopes (Acosta et al., 2015). The key factor at Pima Wash, not factored in Amundson et al. (2015) or Acosta et al. (2015), is the importance of more closely spaced joints that facilitate an increase in grain porosity, that in turn facilitate surface instability and grus production (Fig. 11).

A 3-year study of grus detachment from the crests of ridges in Pima Wash revealed a short-term erosion rate of 0.0310 ± 0.0015 mm/yr, which is equivalent to 31.0 ± 10.5 mm/ka (Dorn, 2015). A study of granite grus trapped behind sediment retention basins between 1986 and 2000 in the nearby granitic Usery Mountains reveal a minimum erosion rate of ~61 mm/ka (Henze, 2000) for an area that has experienced off-road vehicle and other disturbances on the periphery of metropolitan Phoenix. Thus, our CWDR rates (Table 2) are about one-third of disturbed desert drainages and about two-thirds of undisturbed desert hillcrests from the same watershed.

When placed in the context of modern soil erosion rates (García-Ruiz et al., 2015), the 200 mm/yr annual precipitation and ~60 Mg/km^2 average erosion rate of this CWDR study area plots slightly below the average for global study sites analyzed (García-Ruiz et al., 2015). Previous research noted that historic (~a couple of hundred years) gauged stream sediment fluxes can be lower than CWDR measurements that average erosion over the last glacial cycle (Kirchner et al., 2001). That the long-term CWDR displays an opposite trend, lower than historic observations or global expectations, could be a function of some stochastic disturbances along Pima Wash crests increasing erosion rates; or other factors such as armoring in a desert setting might not be as effective as in other regions (Granger et al., 2001).

6.4. No hurricane moisture influence

The broader literature on CWDR contains few examples of the effects of singular extreme high-magnitude, low-frequency events on the CWDR signal. Our initial CWDR sampling occurred prior to a 500-year precipitation event and flood at South Mountains on 8 September, 2014 associated with remnant moisture from Hurricane Norbert. The event started with 87 mm/h precipitation, and then another 68 mm fell over the next 285 min — producing the wettest day on record in Phoenix, Arizona.

Resampling two locations after the flooding resulted in no change in the CWDR at either site (Table 1). The similarity in CWDR before and after a 500-year flooding event may indicate that hurricane moisture-moved sediments with low concentrations of ^{10}Be stayed in upland portions of the basin and did not move all of the way to the main channel (Rickenmann and Zimmermann, 1993; Kober et al., 2012). Most sediments in the study area were produced mainly by grain detachment or shallow (≪60 cm) spalling, and overland flow is the most dominant transportation mechanism (Dorn, 2015). Thus, the lack of change in CWDR before and after a 500-year event suggests that arid granite hillslope sediment transport involves a series of short-distance, stop-and-go, and changes in position — at least in this Sonoran Desert small watershed. We also note that our study confirms the average representativeness of CWDR as a long-term denudation proxy (von Blanckenburg, 2005).

6.5. Pima Wash incision rates

The recorded phase of main channel incision started about 60 ka (Fig. 13). This incision led to fill terraces in the piedmont embayment (Fig. 14) and exposed bedrock outcrops inside the terrace risers that were once buried by alluvium. While we cannot rule out two sudden downcutting events creating the two mapped terrace surfaces, the long-term rate of wash incision appears to be on the order of ~70–180 mm/ka. Although no prior research exists on incision into the terraces of mountain ranges in south-central Arizona, these rates, however, would be compatible with the expected behavior of both occasional rapid incision that is stuck by a resistant barrier and the following lateral erosion seen in numerical models for streams in larger metamorphic core complexes in southern Arizona (Pelletier et al., 2009). Alternatively, fluvial incision rates 4–10 times higher than CWDR could have been caused by an increase in precipitation during the wetter last glacial period (Lozano-García and Ortega-Guerrero, 2002).

6.6. Jointing and the emergence of domed inselbergs

We found little evidence of knickpoint erosion. Only two out of the 32 knickpoint flutes reveal any evidence of erosion in the last quarter century of direct observations. A representative 7-m knickpoint sampled for ^{10}Be surface exposure dating recorded no detectable difference between the portion of the low dome abraded by Pima Wash and

adjacent control sites on the bedrock dome (Fig. 6). The apparent stability of these knickpoints with wide joint spacing facilitates the maintenance of a sequence of strath floodplains immediately above knickpoints, followed by sandy sections that terminate at the next upstream knickpoint. These observations fit well with prior conclusions on the formation of strath floodplains in small arid granitic watersheds (Larson and Dorn, 2014).

The erosion rates of one low dome of ~4.5 to 8.5 mm/ka are similar to granite inselbergs in the Namib Desert (Cockburn et al., 1999) and bedrock granite surfaces in arid Australia (Heimsath et al., 2001; Biermen and Caffee, 2002). This low dome's erosion rate is about one-third to -fourth of CWDR, and thus granitic dome growth could lead to generation (Twidale, 1982) of the observed castle koppie and nubbin forms.

Stepped topography works under the assumption that minimally jointed, bare granite (steps) decay slower than the surrounding soil-mantled granite (tread) (Wahrhaftig, 1965). Subsequent research in Wahrhaftig's southern Sierra Nevada study area reveals that bare bedrock can erode more slowly and also sometimes faster than the surrounding soil-mantled topography (Jessup et al., 2011). What we observe at Pima Wash is somewhat similar to Wahrhaftig's (1965) original hypothesis of differential erosion, where a low dome serves as a knickpoint, and its erosion rate is one-third of the surrounding catchment erosion. Based on this single case study, we speculate that the stability of the studied 7-m Pima Wash knickpoint would facilitate the formation of an upstream step and strath floodplain development behind the step — that is until Pima Wash shifts laterally and is able to access weaker substrate for downcutting. Pelletier et al. (2009, p. 382) notes this possibility, that their model for the Catalina metamorphic core complex in Arizona would yield longitudinal profiles that exhibit random walk-like behavior for snapshots in time, but knickpoints would shift laterally over time as new heterogeneities are exhumed. This point is particularly clear when considering the nature of alluvial storage in the model and in actual profiles. The pattern of knickzones associated with low granitic domes at Pima Wash is consistent with this modeled possibility.

7. Conclusion

This paper explores whether or not the innovative concept linking geomorphology and ecosystem dynamics termed process domains (Montgomery, 1999) can be applied to a common setting in deserts: tiny drainage basins with an area <5 km^2 with a granitic lithology. The Pima Wash watershed in the Sonoran Desert has flora and fauna typical of the Sonoran Desert and hosts a suite of granitic landforms such as kopjes and low domes.

Our primary finding is that process domains offer new insights into geomorphic influences on the ecology of desert watersheds. This study identifies four process domains: (PD1) armored drainage divides; (PD2) slopes mixing different granite landforms; (PD3) mid and upper basin channels that mix knickzones, strath floodplains, and sandy alluvial sections; and (PD4) the main ephemeral channel transitioning to the piedmont.

In PD1, where three years of sediment trap data reveal that drainage divides have been eroding at 31.0 ± 10.5 mm/ka (Dorn, 2015), water flow moves off bedrock surfaces and enhances the growth of perennial vegetation in this xeric position by funneling water to roots. Then, overland flow moves off crests and down slopes in PD2, where trees like *B. microphylla* prefer wide joint spacing that funnels runoff off bedrock surfaces toward roots; desert shrubs, however, show no preference with respect to jointing. In the ephemeral channels of PD3, overland flow shed by low dome bedrock surfaces enhance plant growth and associated amphibians and insects downstream from knickpoints. In PD4, great moisture contrasts exist between the main Pima channel and adjacent desert pavements on stream terraces, resulting in contrasting vegetation cover. Stage 3 calcretes exposed on terrace walls in PD4 provide roofs for the dens of coyotes and gray fox.

As a generalization, geomorphic processes influenced by joint spacing lead to a mixture of xeric and mesic physical habitats with an irregular distribution on the scale of tens of meters. Bedrock granite shedding water causes pockets of plant abundance and associated fauna. Variations in jointing produce a mixture of bedrock and grus, of extreme moisture deficit adjacent to pockets of moisture availability that can last for weeks after a rain. These moisture pockets produce a diversity of plant and animal life so notable in the Sonoran Desert on slopes (Alcock, 1984) and along ephemeral washes (Jones and Glinski, 1985; Warren and Anderson, 1985; Sandercock et al., 2007; Stromberg et al., 2009a,b)

Acknowledgments

We thank the Phoenix Parks and Recreation Department for permission to collect samples and the Maricopa County Flood Control District for topographic data. This research was supported by the College of Education, Korea University Grant in 2015 for Y.B. Seong (K1519391). Minnesota State University allowed research time and travel for this project. We thank Daniel Krahenbuhl, Michael Davis, Paul Padegimas, Ara Jeong, and Youngeun Kim for their field assistance. Dong Eun Kim is greatly appreciated for his help with GIS analysis.

Map. KMZ file containing the Google map of the most important areas described in this article.

Appendix A. Supplementary data

Supplementary data associated with this article can be found in the online version, at doi:http://dx.doi.org/10.1016/j.geomorph.2015.12.014. These data include Google map of the most important areas described in this article.

References

Abrahams, A.D., Parsons, A.J., Hirsch, P.J., 1985. Hillslope gradient–particle size relations: evidence of the formation of debris slopes by hydraulic processes in the Mojave Desert. J. Geol. 93, 347–357.

Acosta, V.T., Schildgen, T.F., Clarke, B.A., Scherler, D., Bookhagen, B., Wittmann, H., von Blanckenburg, F., Strecker, M.R., 2015. Effect of vegetation cover on millennial-scale landscape denudation rates in East Africa. Lithosphere 7, 408–420.

Alcock, J., 1984. Sonoran Desert Spring. University of Arizona Press, Tucson.

Allen, C., Swetnam, T., Betancourt, J., 1998. Landscape changes in the southwestern United States: techniques, long-term data sets, and trends. In: Sisk, T.D. (Ed.), Perspectives on the Land Use History of North America: A Context for Understanding our Changing Environment. U.S. Geological Survey Biological Resources Division, Biological Science Report USGS/BRD/BSR-1998-0003. U.S. Geological Survey, Reston, p. 104 (See also http://biology.usgs.gov/luhna/chap9.html).

Amundson, R., Heimsath, A.M., Owen, J., Yoo, K., Dietrich, W.E., 2015. Hillslope soils and vegetation. Geomorphology 234, 122–132.

Balco, G., Stone, J.O., Lifton, N.A., Dunai, T.J., 2008. A complete and easily accessible means of calculating surface exposure ages or erosion rates from ^{10}Be and ^{26}Al measurements. Quat. Geochronol. 3, 174–195.

Baron, J.S., LaFrancois, T., Kondratieff, B.C., 1998. Chemical and biological characteristics of desert rock pools in intermittent stream of Capitol Reef National Park, Utah. Great Basin Nat. 53, 250–264.

Becker, R.A., Tikoff, B., Riley, P.R., Iverson, N.R., 2014. Preexisting fractures and the formation of an iconic American landscape: Tuolumne Meadows, Yosemite National Park, USA. GSA Today 24 (11). http://dx.doi.org/10.1130/GSATG1203A.1131.

Bellmore, J.R., Baxter, C.V., 2014. Effects of geomorphic process domains on river ecosystems: a comparison of floodplain and confined valley segments. River Res. Appl. 30, 617–630.

Biermen, P., Caffee, M., 2002. Cosmogenic exposure and erosion history of Australian bedrock landforms. Geol. Soc. Am. Bull. 114, 787–803.

von Blanckenburg, F., 2005. The control mechanisms of erosion and weathering at basin scale from cosmogenic nuclides in river sediment. Earth Planet. Sci. Lett. 237, 462–479.

Brardinoni, F., Hassan, M.A., 2006. Glacial erosion, evolution of river long profiles, and the organization of process domains in mountain drainage basins of coastal British Columbia. J. Geophys. Res. Earth Surf. 111, F01013 (doi:01010.01029/02005JF000358).

Büdel, J., 1982. Climatic Geomorphology. Translated by Lenore Fischer and Detlef Busche. Princeton University Press, Princeton, New Jersey.

Cervantes, J.H.F., Istanbullouglu, E., Vivoni, E.R., Collins, C.D.H., Bras, R.L., 2014. A geomorphic perspective on terrain-modulated organization of vegetation productivity:

analysis in two semiarid grassland ecosystems in Southwestern United States. Ecohydrology 7, 242–257.
Chmeleff, J., von Blanckenburg, F., Kossert, K., Jakob, D., 2010. Determination of the ^{10}Be half-life by multicollector ICP-MS and liquid scintillation counting. Nucl. Instrum. Methods Phys. Res. Sect. B Beam Interact. Mater. Atoms 268, 192–199.
Clapp, E.M., Biermen, P.R., Schick, A.P., Lekach, J., Enzel, Y., Caffee, M., 2000. Sediment yield exceeds sediment production in arid region drainage basins. Geology 28, 995–998.
Cockburn, H.A.P., Seidl, M.A., Summerfield, M.A., 1999. Quantifying denudation rates on inselbergs in the central Namib Desert using in situ-produced cosmogenic Be-10 and Al-26. Geology 27, 399–402.
Collins, B.D., Montgomery, D.R., 2011. The legacy of Pleistocene glaciation and the organization of lowland alluvial process domains in the Puget Sound region. Geomorphology 126, 174–185.
Cooke, R.U., Warren, A., 1973. Geomorphology in Deserts. University of California Press, Berkeley.
Derbyshire, E. (Ed.), 1976. Geomorphology and Climate. Wiley, London.
Dorn, R.I., 1995. Digital processing of back-scatter electron imagery: a microscopic approach to quantifying chemical weathering. Geol. Soc. Am. Bull. 107, 725–741.
Dorn, R.I., 1998. Rock coatings. Elsevier, Amsterdam.
Dorn, R.I., 2015. Impact of consecutive extreme rainstorm events on particle transport: case study in a Sonoran Desert range, western USA. Geomorphology 250, 53–62.
Ehlen, J., 1992. Analysis of spatial relationships among geomorphic, petrographic and structural characteristics of the Dartmoor tors. Earth Surf. Process. Landf. 17, 53–67.
Ehlen, J., 1999. Fracture characteristics in weathered granites. Geomorphology 31, 29–45.
Etchberer, R.C., Krausman, P.R., 1997. Evaluation of five methods for measuring desert vegetation. Wildl. Soc. Bull. 25, 604–609.
Eyles, N., Arnaud, E., Scheidegger, A.E., Eyles, C.H., 1997. Bedrock jointing and geomorphology in southwestern Ontario, Canada: an example of tectonic predesign. Geomorphology 19, 17–34.
Fitzgerald, P.G., Reynolds, S.J., Stump, E., Foster, D.A., Gleadow, A.J.W., 1993. Thermochronologic evidence for timing of denudation and rate of crustal extension of the South Mountains metamorphic core complex and Sierra Estrella, Arizona. Nucl. Tracks Radiat. Meas. 21, 555–563.
Flint, J.J., 1974. Stream gradient as a function of order, magnitude, and discharge. Water Resour. Res. 10, 969–973.
Foster, D.A., Gleadow, A.J.W., Reynolds, S.J., Fitzgerald, P.G., 1993. Denudation of metamorphic core complexes and the reconstruction of the transition zone, West central Arizona: constraints from apatite fission track thermochronology. J. Geophys. Res. Solid Earth 98, B2167–B2184.
García-Ruiz, J.M., Beguería, S., Nadal-Romero, E., González-Hidalgo, J.C., Lana-Renault, N., Sanjuán, Y., 2015. A meta-analysis of soil erosion rates across the world. Geomorphology 239, 160–173.
Gordon, S.J., Brady, P.V., 2002. In situ determination of long-term basaltic glass dissolution in the unsaturated zone. Chem. Geol. 90, 115–124.
Graf, W.L., 1988. Fluvial Processes in Dryland Rivers. Springer-Verlag, Berlin.
Granger, D.E., Riebe, C.S., Kirchner, J.W., Finkel, R.C., 2001. Modulation of erosion on steep granitic slopes by boulder armoring, as revealed by cosmogenic Al-26 and Be-10. Earth Planet. Sci. Lett. 186, 269–281.
Grubbs, S.E., Krausman, P.R., 2009. Use of urban landscape by coyotes. Southwest. Nat. 54, 1–12.
Gudmundsdottir, M.H., Blisniuk, K., Ebert, Y., Levine, N.M., Rood, D.H., Wilson, A., Hilley, G.E., 2013. Restraining bend tectonics in the Santa Cruz Mountains, California, imaged using ^{10}Be concentrations in river sands. Geology 41, 843–846.
Gutierrez, M., 2005. Climatic Geomorphology. Elsevier, Amsterdam.
Hamdan, A., 2012. Biogeomorphological effects of the Central Arizona Project (CAP) Canal on a small ephemeral wash near Apache Junction, Arizona. Phys. Geogr. 33, 183–204.
Hassan, M.A., 1990. Scour, fill and burial depth of coarse material in gravel bed streams. Earth Surf. Process. Landf. 15, 341–356.
Heimsath, A.M., Chappell, J., Dietrich, W.E., Nishiizumi, K., Finkel, R., 2001. Late Quaternary erosion in southeastern Australia: a field example using cosmogenic nuclides. Quat. Int. 83–85, 169–185.
Heisinger, B., Lal, D., Kubik, P., Ivy-Ochs, S., Knie, K., Nolte, E., 2002a. Production of selected cosmogenic radionuclides by muons: 2. Capture of negative muons. Earth Planet. Sci. Lett. 200, 357–369.
Heisinger, B., Lal, D., Kubik, P., Ivy-Ochs, S., Neumaier, S., Knie, K., Lazarev, V., Nolte, E., 2002b. Production of selected cosmogenic radionuclides by muons: 1. Fast muons. Earth Planet. Sci. Lett. 200, 345–355.
Henze, M.W., 2000. Sediment Yield on Spook Hill Pediment, Arizona (M.S. Thesis) Geography, Arizona State University, Tempe, pp. 1–224.
Howard, A.D., Selby, M.J., 2009. Rock slopes. In: Parsons, A.J., Abrahams, A.D. (Eds.), Geomorphology of Desert Environments. Springer, New York, pp. 189–232.
Hupp, C.R., Osterkamp, W.R., 1996. Riparian vegetation and fluvial geomorphic processes. Geomorphology 14, 277–295.
Ives, R.L., 1965. Interior erosion of desert mountains. J. Geogr. 64, 3–14.
Jessup, B.S., Hahm, W.J., Miller, S.N., Kirchner, J.W., Riebe, C.S., 2011. Landscape response to tipping points in granite weathering: the case of stepped topography in the Southern Sierra Critical Zone Observatory. Appl. Geochem. 26, 548–550.
Jones, K.B., Glinski, P.C., 1985. Microhabitats of lizards in a southwestern riparian community. In: Johson, R.R., Ziebell, C.D., Patton, D.R., Ffolliott, P.F., Hamre, R.H. (Eds.), Riparian Ecosystems and Their Management: Reconciling Conflicting Uses. USDA Forest Service, Rocky Mountain Research Stations, General Technical Report RM-120, Fort Collins, CO, pp. 342–346.
Kim, D.E., Seong, Y.B., Byun, J.M., Weber, J., Min, K., 2016. Geomorphic disequilibrium in the Eastern Korean Peninsula: possible evidence for reactivation of a rift-flank margin. Geomorphology 254, 130–145.
Kirchner, J.W., Finkel, R.C., Riebe, C.S., Granger, D.E., Clayton, J.L., King, J.G., Megahan, W.F., 2001. Mountain eroion over 10 yr, 10 k.y., and 10 m.y. time scales. Geology 29, 591–594.
Kober, F., Hippe, K., Salcher, B., Ivy-Ochs, S., Kubik, P.W., Wacker, L., Hählen, N., 2012. Debris-flow-dependent variation of cosmogenically derived catchment-wide denudation rates. Geology 40, 935–938.
Kohl, C.P., Nishiizumi, K., 1992. Chemical isolation of quartz for measurement of in-situ produced cosmogenic nuclides. Geochim. Cosmochim. Acta 56, 3583–3587.
Korschinek, G., Bergmaier, A., Faestermann, T., Gerstmann, U.C., Knie, K., Rugel, G., Wallner, A., Dillmann, I., Dollinger, G., Lierse von Gostomski, C., Kossert, K., Maiti, M., Poutivtsev, M., Remmert, A., 2010. A new value for the half-life of ^{10}Be by heavy-ion elastic recoil detection and liquid scintillation counting. Nucl. Instrum. Methods Phys. Res. Sect. B Beam Interact. Mater. Atoms 268, 187–191.
Lal, D., 1991. Cosmic ray labeling of erosion surfaces: in situ nuclide production rates and erosion models. Earth Planet. Sci. Lett. 104, 424–439.
Larson, P.H., Dorn, R.I., 2014. Strath development in small-arid watersheds: case study of South Mountain, Sonoran Desert, Arizona. Am. J. Sci. 314, 1202–1223.
Laub, B.G., Jimenez, J., Budy, P., 2015. Application of science-based restoration planning to a desert river system. Environ. Manag. 55, 1246–1261.
Legrain, N., Dixon, J., Stüwe, K., von Blanckenburg, F., Kubik, P., 2015. Post-Miocene landscape rejuvenation at the eastern end of the Alps. Lithosphere 7, 3–13.
Lekach, J., Schick, A.P., 1983. Evidence for transport of bedload in waves: analysis of fluvial sediment in a small upland stream channel. Catena 10, 267–279.
Linton, D.L., 1955. The problem of tors. Geogr. J. 121 (470–481 + 487).
Liu, T., 2003. Blind testing of rock varnish microstratigraphy as a chronometric indicator: results on late Quaternary lava flows in the Mojave Desert, California. Geomorphology 53, 209–234.
Liu, T., Broecker, W.S., 2007. Holocene rock varnish microstratigraphy and its chronometric application in drylands of western USA. Geomorphology 84, 1–21.
Liu, T., Broecker, W.S., 2013. Millennial-scale varnish microlamination dating of late Pleistocene geomorphic features in the drylands of western USA. Geomorphology 187, 38–60.
Livers, B., Wohl, E., 2015. An evaluation of stream characteristics in glacial versus fluvial process domains in the Colorado Front Range. Geomorphology 231, 72–82.
Lozano-García, M.S., Ortega-Guerrero, B., Susana, S.-N., 2002. Mid-to Late-Wisconsin pollen record of San Felipe Basin, Baja California. Quat. Res. 58 (1), 84–92(89).
Mabbutt, J.C., 1977. Desert Landforms. Australian National University Press, Canberra.
McAuliffe, J.R., Van Devender, T.R., 1998. A 22,000-year record of vegetation change in the north-central Sonoran Desert. Palaeogeogr. Palaeoclimatol. Palaeoecol. 141, 253–275.
McGinnies, W.C., Goldman, B.J., Paylor, P., 1968. Desert of the World, An Appraisal of Research Into Their Physical and Biological Environments. University of Arizona Press.
Michaud, G.A., Monger, H.C., Anderson, D.L., 2013. Geomorphic–vegetation relationships using a geopedological classification system, northern Chihuahuan Desert, USA. J. Arid Environ. 90, 45–54.
Migon, P., Goudie, A.S., 2003. Granite landforms of the Central Namib. Acta Univ. Carol. Geol. 35, 17–38 (Supplement).
Molnar, P., Anderson, R.S., Andersson, S.P., 2007. Tectonics, fracturing of rock, and erosion. J. Geophys. Res. Earth Surf. 112. http://dx.doi.org/10.1029/2005JF000433.
Montgomery, D.R., 1999. Process domains and the river continuum. J. Am. Water Resour. Assoc. 35, 397–410.
Neeson, T.M., Adlerstein, S.A., Wiley, M.J., 2012. Towards a process domain-sensitive substrate habitat model for Sea Lampreys in Michigan Rivers. Trans. Am. Fish. Soc. 141, 313–326.
Nishiizumi, K., Imamura, M., Caffee, M.W., Southon, J.R., Finkel, R.C., McAninch, J., 2007. Absolute calibration of ^{10}Be AMS standards. Nucl. Instrum. Methods Phys. Res. Sect. B Beam Interact. Mater. Atoms 258, 403–413.
Paradise, T.R., 2013. Tafoni and other rock basins. In: Pope, G.A. (Ed.), Treatise on GeomorphologyWeathering and Soils Geomorphology vol. 4. Academic Press, San Diego, pp. 111–126.
Parker, K.C., 1991. Topography, substrate, and vegetation patterns in the northern Sonoran Desert. J. Biogeogr. 18, 151–163.
Parsons, A.J., Abrahams, A.D., 1987. Gradient–particle size relations on quartz monzonite debris slopes in the Mojave Desert. J. Geol. 1987, 423–452.
Parsons, A.J., Abrahams, A.D., Howard, A.D., 2009. Rock-mantled slopes. In: Parsons, A.J., Abrahams, A.D. (Eds.), Geomorphology of Desert Environments. Springer, New York, pp. 233–263.
Pelletier, J.D., Engelder, T., Comeau, D., Hudson, A., Leclerc, M., Youberg, A., Diniega, S., 2009. Tectonic and structural control of fluvial channel morphology in metamorphic core complexes: the example of the Catalina–Rincon core complex, Arizona. Geosphere 5, 363–384.
Polvi, L.E., Wohl, E.E., Merritt, D.M., 2011. Geomorphic and process domain controls on riparian zones in the Colorado Front Range. Geomorphology 125, 504–516.
Reid, I., Laronne, J.B., Powell, D.M., 1995. The Nahal Yatir bedload database: sediment dynamics in a gravel-bed ephemeral stream. Earth Surf. Process. Landf. 20, 845–857.
Reynolds, S.J., 1985. Geology of the South Mountains, Central Arizona. Ariz. Bur. Geol. Miner. Technol. Bull. 195, 1–61.
Rickenmann, D., Zimmermann, M., 1993. The 1987 debris flows in Switzerland: documentation and analysis. Geomorphology 8, 175–189.
Sandercock, P.J., Hooke, J.M., Mant, J.M., 2007. Vegetation in dryland river channels and its interaction with fluvial processes. Prog. Phys. Geogr. 31, 107–129.
Scheidegger, A.E., 2001. Surface joint systems, tectonic stresses and geomorphology: a reconciliation of conflicting observations. Geomorphology 38, 213–219.
Schick, A.P., 1974. Formation and obliteration of desert stream terraces — a conceptual analysis. Zeitschrift fur Geomorphology N.F. Supplement Band 21, pp. 81–105.
Schick, A.P., Lekach, J., 1993. An evaluation of two ten-year sediment budgets, Nahal Yael, Israel. Phys. Geogr. 14, 225–238.

Spencer, J.E., 2000. Possible origin and significance of extension-parallel drainages in Arizona's metamorphic core complexes. Geol. Soc. Am. Bull. 112, 727–735.
St Clair, J., Moon, S., Holbrook, W.S., Perron, J.T., Riebe, C.S., Martel, S.J., Carr, B., Harman, C., Singha, K., Richter, D. deB., 2015. Geophysical imaging reveals topographic stress control of bedrock weathering. Science 350, 534–538.
Stone, J.O., 2000. Air pressure and cosmogenic isotope production. J. Geophys. Res. 105, B23753–B23759.
Stromberg, J.C., Katz, G., 2011. Vegetation structure and function along ephemeral streams in the Sonoran Desert. AGU Fall Meeting Abstracts, p. 1 (04P).
Stromberg, J.C., Hazelton, A.F., White, M.S., 2009a. Plant species richness in ephemeral and perennial reaches of a dryland river. Biodivers. Conserv. 18, 663–677.
Stromberg, J.C., Hazelton, A.F., White, M.S., White, J.M., Fischer, R.A., 2009b. Ephemeral wetlands along a spatially intermittent river: temporal patterns of vegetation development. Wetlands 29, 330–342.
Stromberg, J.C., Boudell, J.A., Hazelton, A.F., 2008. Differences in seed mass between hydric and xeric plants influence seed bank dynamics in a dryland riparian ecosystem. Funct. Ecol. 22, 205–212.
Sutfin, N.A., Shaw, J.R., Wohl, E.E., Coooper, D.J., 2014. A geomorphic classification of ephemeral channels in a mountainous, arid region, southwestern Arizona, USA. Geomorphology 221, 164–175.
Troia, M.J., Williams, L.R., Williams, M.G., Ford, N.B., 2015. The process domains concept as a framework for fish and mussel habitat in a coastal plain river of southeastern North America. Ecol. Eng. 75, 484–496.
Twidale, C.R., 1982. Granite Landforms. Elsevier, Amsterdam.
Twidale, C.R., Bourne, J.A., 1975. The subsurface initiation of some minor granite landforms. J. Geol. Soc. Aust. 22, 477–484.
Van Devender, T.R., 1990. Late Quaternary vegetation and climate of the Sonoran Desert, United States and Mexico. In: Betancourt, J.L., Van Devender, T.R., Martin, P.S. (Eds.), Packrat Middens: The Last 40,000 Years of Biotic Change. University of Arizona Press, Tucson, pp. 134–165.
Viles, H.A., 2013. Linking weathering and rock slope instability: non-linear perspectives. Earth Surf. Process. Landf. 38, 62–70.
Wahrhaftig, C., 1965. Stepped topography of the Southern Sierra Nevada. Geol. Soc. Am. Bull. 76, 1165–1190.
Wainwright, J., 2009. Desert ecogeomorphology. In: Parsons, A.J., Abrahams, A.D. (Eds.), Geomorphology of Desert Environments, second ed. Springer, Amsterdam, pp. 21–66.
Wakatsuki, T., Sasaki, Y., Tanaka, Y., Matsukura, Y., 2007. Predictive equation of unit weights, shear strength parameters and permeability of grus using a simplified dynamic cone penetrometer hardness and grain size. J. Jpn. Soc. Erosion Control Eng. 59, 38–46.
Wallace, J.E., Steidl, R.J., Swann, D.E., 2010. Habitat characteristics of lowland leopard frogs in mountain canyons of southeastern Arizona. J. Wildl. Manag. 74, 808–815.
Warren, P.L., Anderson, L.S., 1985. Gradient analysis of a Sonoran Desert wash. In: Johnson, R.J., Ziebell, C.D., Patton, D.R., Ffolliott, P.F., Hamre, R.H. (Eds.), Riparian Ecosystems and Their Management: Reconciling Conflicting Uses. USDA Forest Service, Tucson, pp. 150–155.
Warren, D.K., Turner, R.M., 1975. Saltcedar (*Tamarix chinensis*) seed production, seedling establishment, and response to inundation. J. Ariz. Acad. Sci. 10, 135–144.
Whipple, K.X., Wobus, C., Crosby, B., Kirby, E., Sheehan, D., 2007. New tools for quantitative geomorphology: extraction and interpretation of stream profiles from digital topographic data. Geological Society of America, Annual Meeting, Short Course Guide: Boulder, Colorado (http://www.geomorphtools.org).
Wohl, E., 2008. The effect of bedrock jointing on the formation of straths in the Cache la Poudre River drainage, Colorado Front Range. J. Geophys. Res. 113, F01007 (doi: 01010.01029/02007JF000817).
Wohl, E., 2010. A brief review of the process domain concept and its application to quantifying sediment dynamics in bedrock canyons. Terra Nova 22, 411–416.
Wohl, E., 2011. What should these rivers look like? Historical range of variability and human impacts in the Colorado Front Range, UGS. Earth Surf. Process. Landf. 36, 1378–1390.
Wohl, E., 2014. Dryland channel networks: resiliency, thresholds, and management metrics. Geol. Soc. Am. Rev. Eng. Geol. 22, 147–158.
Wohl, E.E., Merritt, D.M., 2001. Bedrock channel morphology. Geol. Soc. Am. Bull. 113, 1205–1212.
Wondzell, S.M., Cunningham, G.L., Bachelet, D., 1996. Relationships between landforms, geomorphic processes, and plant communities on a watershed in the northern Chihuahuan Desert. Landsc. Ecol. 11, 351–362.
Wu, H., Pollard, D.D., 1995. An experimental study of the relationship between joint spacing and layer thickness. J. Struct. Geol. 17, 887–905.
Yair, A., Kossovsky, A., 2002. Climate and surface properties: hydrologic response of small arid and semi-arid watersheds. Geomorphology 42, 43–57.
Young, R., Young, A.R.M., 1992. Sandstone Landforms. Springer-Verlag, Berlin.